the roles of ion transporters, which are greatly affected by ion concentrations.

The model of I_{NaK} in the FP model was largely modified from the original model of Chapman et al. (1983) by omitting state transitions of the carrier protein. This simplification resulted in no saturation of the turnover rate by $[Na^+]_i$. Moreover, I_{NaK} in the FP model is a V-independent current in the range from −80 to 0 mV. We implemented a new kinetic model of I_{NaK} with the state transitions (Oka et al., 2010). It shows properties well established in experimental studies, such as dependencies on Na^+ and K^+, the free energy of ATP hydrolysis (ΔG_{ATP}), and the membrane potential. Thereby, the present study reliably predicted that I_{NaK} took a pivotal role in terminating the burst when $[Na^+]_i$ was accumulated during a long-lasting burst at a high [G] (Fig. 5). For comparison with the present study, we applied V_L analysis to the slow interburst depolarization in the FP model (Fig. S4). At a relatively low [G] (8.5 mM), a V_L diagram demonstrated that the time-dependent decrease of outward I_{NaK} takes the major role in determining the depolarization rate ($c \sim 0.25$ mV s^{-1}), whereas the contribution of I_{KATP} was negligibly small ($c \sim 0.025$ mV s^{-1}). It is because of a relatively rapid production of ATP in the FP model, resulting in a long-lasting burst even at relatively lower [G], accompanied by $[Na^+]_i$ oscillation with an amplitude of ~2 mM.

Mechanisms to generate the bursting activity in modeling studies

Complex patterns of electrical activity in β cells with varying [G] has been one of the interesting targets in the field of mathematical physiology, and several explicit hypotheses have been put forward in various forms of mathematical models. Importantly, however, the fundamental question still remained as to what the slowly varying factor underlying the time course of burst–interburst rhythm in β cells is. Here, we discuss the multiple key membrane components suggested in relation to the slow intracellular factors hypothesized in previous modeling studies, that is, $[Ca^{2+}]_i$, $[Ca^{2+}]_{ER}$, [ATP] and/or [ADP], and $[Na^+]_i$.

$[Ca^{2+}]$ and the Ca^{2+}-activated K^+ currents. One of the major hypotheses assumed a gradual activation of Ca^{2+}-dependent K^+ currents during an action potential burst. For example, early Chay-Keizer models adopted the BK channel (Chay and Keizer, 1983; Sherman et al., 1988), and they predicted that an accumulation of intracellular Ca^{2+} via repetitive spikes increased the outward BK current and terminated the burst. In turn, the burst was resumed when the BK channels were sufficiently deactivated during the interburst period. Distinct from the expectation in their models, however, the progressive accumulation of Ca^{2+} has not been established experimentally, but rather, a rapid rise of the Ca^{2+} transient leveled off to the plateau level within the initial several seconds of the burst (Santos et al., 1991; Worley et al., 1994a), or $[Ca^{2+}]_i$ slightly rose (Gilon and Henquin, 1992; Zhang et al., 2003) or decayed (Miura et al., 1997; Henquin et al., 2009; Merrins et al., 2010) thereafter. In recent studies, an existence of a different type of Ca^{2+}-dependent K^+ channel, I_{Kslow}, has been reported (Göpel et al., 1999a; Goforth et al., 2002; Zhang et al., 2005).

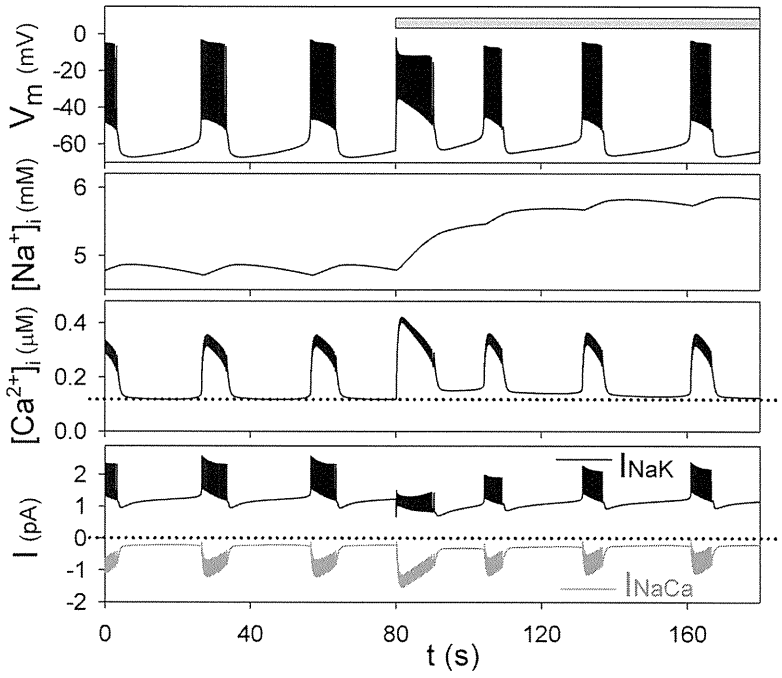

Figure 7. Effects of the inhibition of Na^+/K^+ ATPase by glucose. The inhibition of NaK by glucose was introduced from 80 s (gray bar) by changing F_{glu} (Eq. S55) from 1 to 0.552 at 8 mM [G]. The panels show time courses of V_m, $[Na^+]_i$, $[Ca^{2+}]_i$, I_{NaK}, and I_{NaCa}. Dotted lines indicate the initial basal level of $[Ca^{2+}]_i$ (third panel) and zero current levels (bottom panel).

The important role of I_{Kslow} in terminating the burst via $[Ca^{2+}]$ accumulation was suggested by two mathematical models (Goforth et al., 2002; Fridlyand et al., 2009). To simulate the expected slow kinetics of I_{Kslow}, Goforth et al. (2002) assumed a localized subspace with a substantial volume (occupying ~30% of the cytosolic volume), in which the Ca^{2+} concentration activating I_{Kslow} varies in parallel to changes in $[Ca^{2+}]_{ER}$, rather than the more rapid variation of $[Ca^{2+}]_i$. However, such kinetic changes in I_{Kslow} during the bursting activity nor any histological evidence to justify the diffusion barrier have been found experimentally. Alternatively, Fridlyand et al. (2010) assumed I_{KCas} with an extremely slow time constant of 2.3 s for activation to represent I_{Kslow}. However, SK channels, one of the candidates contributing to the experimental I_{Kslow}, show very fast gating kinetics (Hirschberg et al., 1998).

The slow decay phase of $[Ca^{2+}]_i$ after the burst might lead to slow changes in membrane conductances of several Ca^{2+}-activated channels or transporters. Indeed, the present study suggests that $[Ca^{2+}]_i$ might play a significant role in driving slow interburst depolarization through I_{PMCA}, I_{NaCa}, and I_{TRPM}, as well as $I_{KCa(SK)}$ (Fig. 5). Unfortunately, only a few indirect measurements of these currents have been reported experimentally. As a result, the contribution of I_{TRPM} was only considered in our model, and I_{NaCa} and I_{PMCA} were implemented in a few previous models (Fridlyand et al., 2003; Diederichs, 2006; Meyer-Hermann, 2007).

$[Ca^{2+}]_{ER}$ and I_{SOC}. Repetitive empting and refilling of ER is closely related to bursting rhythm by modulating Ca^{2+}-activated currents. Among them, a store-operated inward current, I_{SOC} (sometimes termed I_{CRAC} or I_{CRAN}), would be a primary candidate to generate the bursting rhythm. Gilon et al. (1999) suggested that ER fills with Ca^{2+} during the burst, and the gradual deactivation of I_{SOC} may lead to termination of the burst. Conversely, the subsequent emptying of the ER after the burst might then reactivate I_{SOC} to trigger a new burst. This mechanism has been tested in several models (Bertram et al., 1995a; Chay, 1996, 1997; Mears et al., 1997; Fridlyand et al., 2003). However, the half-activation concentration of $[Ca^{2+}]_{ER}$ ($K_{0.5,ER}$) has not been measured experimentally, and thus the predicted contributions of I_{SOC} are different among studies. For example, in the models of Chay (1996, 1997) using a $K_{0.5,ER}$ of 50 or 70 µM, the gating of I_{SOC} took a central role in determining the burst rhythm. On the other hand, in the other models I_{SOC} contributed little because the channel remained closed as a result of the assumption of a relatively low $K_{0.5,ER}$ (3 µM; Bertram et al., 1995a, and the present model), or was always open because of an assumed high $K_{0.5,ER}$ (200 µM; Fridlyand et al., 2003). Therefore, it is important for $K_{0.5,ER}$ to be determined experimentally to decide the role of I_{SOC} in generating glucose-induced bursting rhythm under normal conditions. Interestingly, rather consistent effects (the prolongation of the spike burst or the acceleration of the bursting rhythm) were reconstructed with these differing models when I_{SOC} was maximally activated by ER depletion under thapsigargin, muscarinic antagonist, or low glucose (Bertram et al., 1995a; Mears et al., 1997; Fridlyand et al., 2003; the present model).

[ATP] and [ADP] and I_{KATP}. [ATP] and/or [ADP] have been considered as key slow factors, and several β-cell models examined the time-dependent gating of K_{ATP} channels. However, quantitative estimation of the contribution of I_{KATP} to burst activity is highly dependent on the formulation of both I_{KATP} and the metabolic components of each model. For example, Magnus and Keizer (1998) developed a detailed I_{KATP} model and concluded it was a major factor, whereas simulations using the FP model and the same I_{KATP} formulation concluded that I_{KATP} was not of major significance. This is because the two models adopted radically different schemes describing the production of [ATP] and [MgADP].

In addition, it should be noted that ATP-consuming transporters, such as PMCA, SERCA, and NaK, should influence the bursting rhythm by modulating their activities according to the intracellular energy level. However, few studies have dealt with this subject, except the present model by incorporating the detailed kinetic model of I_{NaK} with ΔG_{ATP} dependency.

$[Na^+]_i$ and I_{NaK}. As demonstrated here and in previous modeling studies (Miwa and Imai, 1999; Fridlyand et al., 2003; Meyer-Hermann, 2007), glucose-induced fluctuations of I_{CaV} results in rhythmical Na^+ entry through the action of NCX. Increased $[Na^+]_i$ will activate I_{NaK} and lead to termination of the burst; in turn, a slow decay of $[Na^+]_i$ leads to a decrease in I_{NaK} during the interburst period. Experimentally, Grapengiesser (1996, 1998) observed distinct oscillations of $[Na^+]_i$ under a partial suppression of NaK in mouse β cells. In support of this idea, these oscillations disappeared after inhibition of I_{CaV} or under a lower glucose, but they were insensitive to a blocker of V-dependent Na^+ channels.

$[Na^+]_i$ also modulates the turnover rate of the NCX exchanger. Thus, a proper Na^+ dependency of I_{NaCa} is essential for examination of the role of $[Na^+]_i$ in generating bursting activity. The kinetic scheme of I_{NaCa} used in this study was developed in cardiac cells and has been well tested experimentally. In addition, the tetrodotoxin-sensitive Na^+ current (I_{Na}) might also contribute to intracellular Na^+ accumulation. In preliminary studies, we implemented I_{Na} based on recordings in pancreatic β cells from rat (Hiriart and Matteson, 1988), mouse (Göpel et al., 1999b; Vignali et al., 2006), and human (Braun et al., 2008). However, because I_{Na} was almost completely inactivated at the physiological V_m, the

generated flux was trivial. V_L analysis also revealed that I_{Na} made a very minor contribution to the slow depolarization. Thus, I_{Na} was deleted from the present model.

The $[Na^+]_i$ of 10–14 mM recorded by Grapengiesser (1996) is much higher than the 5.5–7.5 mM in our simulations. When examined with our model, however, 10–14 mM $[Na^+]_i$ resulted in the reverse mode of the NCX all through the normal burst activity because the Na^+-driving force is much reduced. Furthermore, the amplitude of the oscillation of $[Na^+]_i$ and the corresponding effect on I_{NaK} were reliably estimated in our study. This is because the average Na^+ influx through the NCX was determined by the amplitude of I_{CaV} and the action potential frequency, both of which were consistent with experimental data.

Is a single β cell capable of generating full-sized action potentials?

Remarkably, the action potential parameters in our model are quite comparable to experimental measurements in isolated mouse β cells obtained by Smith et al. (1990a) (see Slow fluctuations in [ATP]... in Results). In most papers, however, the amplitude of action potentials was smaller and the quiescent potential less negative when recorded in single β-cell preparations (Rorsman and Trube, 1986; Santos et al., 1991; Kinard et al., 1999; Bertram et al., 2000). It is conceivable that the action potentials might be damped under the patch-clamp recording because the current leak through the gigaseal (~10 GΩ) between the patch electrode and the cell membrane is comparable to the whole cell membrane current (input resistance of ~10–30 GΩ). The membrane capacitance of ~6 pF of small β cells is also in the same order as the floating capacitance of the electrode tip. Moreover, recovery from dissociation injury might be incomplete in culture medium, or action potential generation might be depressed at room temperature or by the rundown of I_{CaV}. It should be noted that mouse or human β cells contain a relatively high density of I_{CaV} ranging over 6 to 11.4 pA pF^{-1}, with an apparent reversal potential of ~50 mV at physiological $[Ca^{2+}]_o$ (see Table I for references). The current densities of I_{CaV} guarantee a fast rising phase and a full size of the action potential in an intact cell before patch-clamp recording. In the present model, the action potential peak was shifted to positive potentials when the membrane K^+ conductance was partially blocked, in agreement with experiments (Atwater et al., 1979; Santos and Rojas, 1989; Rorsman et al., 1992; Houamed et al., 2010). In addition to the action potential amplitude, it should also be noted that the burst duration in single-cell preparations might be affected by the leak conductance and floating capacitance during patch recordings. The difference between electrical activities in single cells and those of islets might be caused by the above recording artifacts.

Further considerations and limitations of the study

The V_L diagram in Fig. 5 indicated prominently large contributions of I_{CaV} during the whole interburst period at both 8 and 16 mM [G]. These contributions are mainly attributable to the increase or decrease in d_{CaV}, which is a pure voltage-dependent gate of I_{CaV}. From the viewpoint that burst–interburst rhythm is principally generated by slow changes in cytosolic substrate concentrations, the role of d_{CaV} is to magnify changes in V_m in the same direction as those induced by other membrane currents under the influence of cytosolic factors. Namely, at 8 mM [G], the slow depolarization induced by changes in I_{KATP} and I_{NaCa} increases d_{CaV}, which results in further depolarization. In the early half of the interburst period at 16 mM [G], d_{CaV} is decreased as a result of the negative shift of V_m, which is primarily induced by a decrease in I_{NaCa} or I_{TRPM} via the progressive decay of $[Ca^{2+}]_i$. During the late phase, the gradual positive shift in V_m induced by a decrease in I_{PMCA} or I_{NaK} increases d_{CaV} to enhance the depolarization. If these secondary contributions of I_{CaV} are excluded from comparison of the membrane currents, the V_L diagram indicates that I_{KATP} and I_{NaCa} at 8 mM [G], and I_{NaCa}, I_{PMCA}, I_{TRPM}, and I_{NaK} at 16 mM [G], play major roles in converting variations in the slow cytosolic factors into the V_m change in our model.

The effects of thapsigargin on $[Ca^{2+}]_i$ have been examined in several experiments using islet preparations, because blocking the ER might provide important clues as to the role of Ca^{2+} buffering by the ER in the bursting rhythm. Unfortunately, there have been no experimental data showing the effects of thapsigargin on the electrical activity or on Ca^{2+} fluctuations in isolated individual β cells. In our single-cell model, the simulation of applying thapsigarin (Fig. 3) was consistent with the accelerated rhythm of the Ca^{2+} fluctuations recorded in several experimental observations in pancreatic islets (Miura et al., 1997; Gilon et al., 1999; Fridlyand et al., 2003), provided that the rhythm of Ca^{2+} transient reflects the electrical

TABLE I

Measurements of the peak of I_{CaV}

Amplitude of I_{CaV}	External solution (mM Ca^{2+})	Species	Reference
51 pA (8.28 pA pF^{-1a})	2.6	mouse	Rorsman et al., 1992
37 pA (6.00 pA pF^{-1a})	2.6	mouse	Islam et al., 1995
70 pA (11.37 pA pF^{-1a})	2.6	mouse	Vignali et al., 2006
93 pA	2.6	mouse	Göpel et al., 1999b
135 pA (21.92 pA pF^{-1a})	10	mouse	Gilon et al., 1997
16 pA pF^{-1}	10	mouse	Arkhammar et al., 1994
16 pA pF^{-1}	10	mouse	Ämmälä et al., 1992
17 pA pF^{-1}	10.2	mouse	Bokvist et al., 1991
6.5 pA pF^{-1}	5	human	Kelly et al., 1991
7 pA pF^{-1}	2.6	human	Braun et al., 2008

[a]Current density.

bursting activity even in the islet preparations. However, it should be noted that in other islet studies, thapsigargin induced a sustained increase in $[Ca^{2+}]_i$ (Worley et al., 1994b; Gilon et al., 1999; Kanno et al., 2002), accompanied by a continuous firing of action potentials (Worley et al., 1994b). Furthermore, both of these responses have been observed in the same experimental study (Miura et al., 1997). At present, it might be speculated that our cell model represents only a given population of β cells, or that the cell-to-cell electrical coupling among different populations of cell types within the islet can produce different patterns in the thapsigargin response.

Although the current system was much improved compared with the previous β-cell models by adding individual current components in the molecular level, further refinement of the formulation will be necessary according to new experimental data in future, especially in respect to temperature effects on channel kinetics. Furthermore, compared with the electrophysiological formulations, the description of energy metabolism is quite simplified in our β-cell model. Therefore, it is beyond the scope of this study to reproduce an ultraslow bursting rhythm with periods >5 min, which have been suspected to be of metabolic origin (Henquin et al., 1982; Bertram et al., 2004). Moreover, the effect of $[Ca^{2+}]_i$ on ATP production was not considered in our model. Keizer and Magnus (1989) assumed that Ca^{2+} entry into the mitochondria depolarized the matrix membrane to inhibit ATP production. However, the opposite effect has also been proposed, namely that an increase in $[Ca^{2+}]_i$ might facilitate ATP production by activating dehydrogenases within the TCA cycle (Cortassa et al., 2003). The net effect of $[Ca^{2+}]_i$ on ATP production is not quantitatively known at present. Therefore, it will be important to include more precise models for glycolysis (Smolen, 1995; Bertram et al., 2004), TCA cycle, and oxidative phosphorylation (Dzbek and Korzeniewski, 2008) in future formulations.

We thank Professor T. Powell for fruitful discussion and for improving the English of this paper.

This work was supported by the Biomedical Cluster Kansai project; a Grant-in-Aid (22590216 to C.Y. Cha and 22390039 to A. Noma) from the Ministry of Education, Culture, Sports, Science and Technology of Japan; and the Ritsumeikan-Global Innovation Research Organization at Ritsumeikan University.

Lawrence G. Palmer served as editor.

Submitted: 7 February 2011
Accepted: 7 June 2011

REFERENCES

Ämmälä, C., P.O. Berggren, K. Bokvist, and P. Rorsman. 1992. Inhibition of L-type calcium channels by internal GTP [gamma S] in mouse pancreatic beta cells. *Pflugers Arch.* 420:72–77. doi:10.1007/BF00378643

Antunes, C.M., A.P. Salgado, L.M. Rosário, and R.M. Santos. 2000. Differential patterns of glucose-induced electrical activity and intracellular calcium responses in single mouse and rat pancreatic islets. *Diabetes.* 49:2028–2038. doi:10.2337/diabetes.49.12.2028

Arkhammar, P., L. Juntti-Berggren, O. Larsson, M. Welsh, E. Nånberg, A. Sjöholm, M. Köhler, and P.O. Berggren. 1994. Protein kinase C modulates the insulin secretory process by maintaining a proper function of the beta-cell voltage-activated Ca^{2+} channels. *J. Biol. Chem.* 269:2743–2749.

Ashcroft, F.M., and M. Kakei. 1989. ATP-sensitive K^+ channels in rat pancreatic beta-cells: modulation by ATP and Mg^{2+} ions. *J. Physiol.* 416:349–367.

Ashcroft, F.M., and P. Rorsman. 1989. Electrophysiology of the pancreatic beta-cell. *Prog. Biophys. Mol. Biol.* 54:87–143. doi:10.1016/0079-6107(89)90013-8

Ashcroft, F.M., D.E. Harrison, and S.J. Ashcroft. 1984. Glucose induces closure of single potassium channels in isolated rat pancreatic beta-cells. *Nature.* 312:446–448. doi:10.1038/312446a0

Atwater, I., B. Ribalet, and E. Rojas. 1979. Mouse pancreatic beta-cells: tetraethylammonium blockage of the potassium permeability increase induced by depolarization. *J. Physiol.* 288:561–574.

Bertram, R., and A. Sherman. 2004. A calcium-based phantom bursting model for pancreatic islets. *Bull. Math. Biol.* 66:1313–1344. doi:10.1016/j.bulm.2003.12.005

Bertram, R., M.J. Butte, T. Kiemel, and A. Sherman. 1995a. Topological and phenomenological classification of bursting oscillations. *Bull. Math. Biol.* 57:413–439.

Bertram, R., P. Smolen, A. Sherman, D. Mears, I. Atwater, F. Martin, and B. Soria. 1995b. A role for calcium release-activated current (CRAC) in cholinergic modulation of electrical activity in pancreatic beta-cells. *Biophys. J.* 68:2323–2332. doi:10.1016/S0006-3495(95)80414-5

Bertram, R., J. Previte, A. Sherman, T.A. Kinard, and L.S. Satin. 2000. The phantom burster model for pancreatic beta-cells. *Biophys. J.* 79:2880–2892. doi:10.1016/S0006-3495(00)76525-8

Bertram, R., L. Satin, M. Zhang, P. Smolen, and A. Sherman. 2004. Calcium and glycolysis mediate multiple bursting modes in pancreatic islets. *Biophys. J.* 87:3074–3087. doi:10.1529/biophysj.104.049262

Bokvist, K., C. Ämmälä, P.O. Berggren, P. Rorsman, and K. Wåhlander. 1991. Alpha 2-adrenoreceptor stimulation does not inhibit L-type calcium channels in mouse pancreatic beta-cells. *Biosci. Rep.* 11:147–157. doi:10.1007/BF01182483

Bozem, M., and J.C. Henquin. 1988. Glucose modulation of spike activity independently from changes in slow waves of membrane potential in mouse B-cells. *Pflugers Arch.* 413:147–152. doi:10.1007/BF00582524

Braun, M., R. Ramracheya, M. Bengtsson, Q. Zhang, J. Karanauskaite, C. Partridge, P.R. Johnson, and P. Rorsman. 2008. Voltage-gated ion channels in human pancreatic beta-cells: electrophysiological characterization and role in insulin secretion. *Diabetes.* 57:1618–1628. doi:10.2337/db07-0991

Brini, M., and E. Carafoli. 2009. Calcium pumps in health and disease. *Physiol. Rev.* 89:1341–1378. doi:10.1152/physrev.00032.2008

Caride, A.J., A.R. Penheiter, A.G. Filoteo, Z. Bajzer, A. Enyedi, and J.T. Penniston. 2001. The plasma membrane calcium pump displays memory of past calcium spikes. Differences between isoforms 2b and 4b. *J. Biol. Chem.* 276:39797–39804. doi:10.1074/jbc.M104380200

Cha, C.Y., Y. Himeno, T. Shimayoshi, A. Amano, and A. Noma. 2009. A novel method to quantify contribution of channels and transporters to membrane potential dynamics. *Biophys. J.* 97:3086–3094. doi:10.1016/j.bpj.2009.08.060

Cha, C.Y., E. Santos, A. Amano, T. Shimayoshi, and A. Noma. 2011. Time-dependent changes in membrane excitability during glucose-induced bursting activity in pancreatic β cells. *J. Gen. Physiol.* 138:39–47.

Chapman, J.B., E.A. Johnson, and J.M. Kootsey. 1983. Electrical and biochemical properties of an enzyme model of the sodium pump. *J. Membr. Biol.* 74:139–153. doi:10.1007/BF01870503

Chay, T.R. 1996. Electrical bursting and luminal calcium oscillation in excitable cell models. *Biol. Cybern.* 75:419–431. doi:10.1007/s004220050307

Chay, T.R. 1997. Effects of extracellular calcium on electrical bursting and intracellular and luminal calcium oscillations in insulin secreting pancreatic beta-cells. *Biophys. J.* 73:1673–1688. doi:10.1016/S0006-3495(97)78199-2

Chay, T.R., and J. Keizer. 1983. Minimal model for membrane oscillations in the pancreatic beta-cell. *Biophys. J.* 42:181–190. doi:10.1016/S0006-3495(83)84384-7

Cheng, H., A. Beck, P. Launay, S.A. Gross, A.J. Stokes, J.P. Kinet, A. Fleig, and R. Penner. 2007. TRPM4 controls insulin secretion in pancreatic beta-cells. *Cell Calcium.* 41:51–61. doi:10.1016/j.ceca.2006.04.032

Chow, R.H., P.E. Lund, S. Löser, U. Panten, and E. Gylfe. 1995. Coincidence of early glucose-induced depolarization with lowering of cytoplasmic Ca^{2+} in mouse pancreatic beta-cells. *J. Physiol.* 485:607–617.

Colsoul, B., A. Schraenen, K. Lemaire, R. Quintens, L. Van Lommel, A. Segal, G. Owsianik, K. Talavera, T. Voets, R.F. Margolskee, et al. 2010. Loss of high-frequency glucose-induced Ca^{2+} oscillations in pancreatic islets correlates with impaired glucose tolerance in Trpm5-/- mice. *Proc. Natl. Acad. Sci. USA.* 107:5208–5213. doi:10.1073/pnas.0913107107

Cook, D.L., and C.N. Hales. 1984. Intracellular ATP directly blocks K^+ channels in pancreatic B-cells. *Nature.* 311:271–273. doi:10.1038/311271a0

Cortassa, S., M.A. Aon, E. Marbán, R.L. Winslow, and B. O'Rourke. 2003. An integrated model of cardiac mitochondrial energy metabolism and calcium dynamics. *Biophys. J.* 84:2734–2755. doi:10.1016/S0006-3495(03)75079-6

Dean, P.M., E.K. Matthews, and Y. Sakamoto. 1975. Pancreatic islet cells: effects of monosaccharides, glycolytic intermediates and metabolic inhibitors on membrane potential and electrical activity. *J. Physiol.* 246:459–478.

Diederichs, F. 2006. Mathematical simulation of membrane processes and metabolic fluxes of the pancreatic beta-cell. *Bull. Math. Biol.* 68:1779–1818. doi:10.1007/s11538-005-9053-9

Düfer, M., B. Gier, D. Wolpers, P. Krippeit-Drews, P. Ruth, and G. Drews. 2009. Enhanced glucose tolerance by SK4 channel inhibition in pancreatic beta-cells. *Diabetes.* 58:1835–1843. doi:10.2337/db08-1324

Dunne, M.J., and O.H. Petersen. 1986. Intracellular ADP activates K^+ channels that are inhibited by ATP in an insulin-secreting cell line. *FEBS Lett.* 208:59–62. doi:10.1016/0014-5793(86)81532-0

Dzbek, J., and B. Korzeniewski. 2008. Control over the contribution of the mitochondrial membrane potential (DeltaPsi) and proton gradient (DeltapH) to the protonmotive force (Deltap). In silico studies. *J. Biol. Chem.* 283:33232–33239. doi:10.1074/jbc.M802404200

Elwess, N.L., A.G. Filoteo, A. Enyedi, and J.T. Penniston. 1997. Plasma membrane Ca^{2+} pump isoforms 2a and 2b are unusually responsive to calmodulin and Ca^{2+}. *J. Biol. Chem.* 272:17981–17986. doi:10.1074/jbc.272.29.17981

Enyedi, A., A.G. Filoteo, G. Gardos, and J.T. Penniston. 1991. Calmodulin-binding domains from isozymes of the plasma membrane Ca^{2+} pump have different regulatory properties. *J. Biol. Chem.* 266:8952–8956.

Fridlyand, L.E., N. Tamarina, and L.H. Philipson. 2003. Modeling of Ca^{2+} flux in pancreatic beta-cells: role of the plasma membrane and intracellular stores. *Am. J. Physiol. Endocrinol. Metab.* 285:E138–E154.

Fridlyand, L.E., L. Ma, and L.H. Philipson. 2005. Adenine nucleotide regulation in pancreatic beta-cells: modeling of ATP/ADP-Ca^{2+} interactions. *Am. J. Physiol. Endocrinol. Metab.* 289:E839–E848. doi:10.1152/ajpendo.00595.2004

Fridlyand, L.E., D.A. Jacobson, A. Kuznetsov, and L.H. Philipson. 2009. A model of action potentials and fast Ca^{2+} dynamics in pancreatic beta-cells. *Biophys. J.* 96:3126–3139. doi:10.1016/j.bpj.2009.01.029

Fridlyand, L.E., N. Tamarina, and L.H. Philipson. 2010. Bursting and calcium oscillations in pancreatic beta-cells: specific pacemakers for specific mechanisms. *Am. J. Physiol. Endocrinol. Metab.* 299:E517–E532. doi:10.1152/ajpendo.00177.2010

Gall, D., J. Gromada, I. Susa, P. Rorsman, A. Herchuelz, and K. Bokvist. 1999. Significance of Na/Ca exchange for Ca^{2+} buffering and electrical activity in mouse pancreatic beta-cells. *Biophys. J.* 76:2018–2028. doi:10.1016/S0006-3495(99)77359-5

Gilon, P., and J.C. Henquin. 1992. Influence of membrane potential changes on cytoplasmic Ca^{2+} concentration in an electrically excitable cell, the insulin-secreting pancreatic B-cell. *J. Biol. Chem.* 267:20713–20720.

Gilon, P., J. Yakel, J. Gromada, Y. Zhu, J.C. Henquin, and P. Rorsman. 1997. G protein-dependent inhibition of L-type Ca^{2+} currents by acetylcholine in mouse pancreatic B-cells. *J. Physiol.* 499:65–76.

Gilon, P., A. Arredouani, P. Gailly, J. Gromada, and J.C. Henquin. 1999. Uptake and release of Ca^{2+} by the endoplasmic reticulum contribute to the oscillations of the cytosolic Ca^{2+} concentration triggered by Ca^{2+} influx in the electrically excitable pancreatic B-cell. *J. Biol. Chem.* 274:20197–20205. doi:10.1074/jbc.274.29.20197

Goforth, P.B., R. Bertram, F.A. Khan, M. Zhang, A. Sherman, and L.S. Satin. 2002. Calcium-activated K^+ channels of mouse β-cells are controlled by both store and cytoplasmic Ca^{2+}: experimental and theoretical studies. *J. Gen. Physiol.* 120:307–322. doi:10.1085/jgp.20028581

Göpel, S.O., T. Kanno, S. Barg, L. Eliasson, J. Galvanovskis, E. Renström, and P. Rorsman. 1999a. Activation of Ca^{2+}-dependent K^+ channels contributes to rhythmic firing of action potentials in mouse pancreatic β cells. *J. Gen. Physiol.* 114:759–770. doi:10.1085/jgp.114.6.759

Göpel, S., T. Kanno, S. Barg, J. Galvanovskis, and P. Rorsman. 1999b. Voltage-gated and resting membrane currents recorded from B-cells in intact mouse pancreatic islets. *J. Physiol.* 521:717–728. doi:10.1111/j.1469-7793.1999.00717.x

Grapengiesser, E. 1996. Glucose induces cytoplasmic Na^+ oscillations in pancreatic beta-cells. *Biochem. Biophys. Res. Commun.* 226:830–835. doi:10.1006/bbrc.1996.1436

Grapengiesser, E. 1998. Unmasking of a periodic Na^+ entry into glucose-stimulated pancreatic beta-cells after partial inhibition of the Na/K pump. *Endocrinology.* 139:3227–3231. doi:10.1210/en.139.7.3227

Hao, L., J.L. Rigaud, and G. Inesi. 1994. Ca^{2+}/H^+ countertransport and electrogenicity in proteoliposomes containing erythrocyte plasma membrane Ca-ATPase and exogenous lipids. *J. Biol. Chem.* 269:14268–14275.

Henquin, J.C. 1990. Role of voltage- and Ca^{2+}-dependent K^+ channels in the control of glucose-induced electrical activity in pancreatic B-cells. *Pflugers Arch.* 416:568–572. doi:10.1007/BF00382691

Henquin, J.C., and H.P. Meissner. 1984a. Effects of theophylline and dibutyryl cyclic adenosine monophosphate on the membrane potential of mouse pancreatic beta-cells. *J. Physiol.* 351:595–612.

Henquin, J.C., and H.P. Meissner. 1984b. Significance of ionic fluxes and changes in membrane potential for stimulus-secretion coupling in pancreatic B-cells. *Experientia.* 40:1043–1052. doi:10.1007/BF01971450

Henquin, J.C., H.P. Meissner, and W. Schmeer. 1982. Cyclic variations of glucose-induced electrical activity in pancreatic B cells. *Pflugers Arch.* 393:322–327. doi:10.1007/BF00581418

Henquin, J.C., M. Nenquin, M.A. Ravier, and A. Szollosi. 2009. Shortcomings of current models of glucose-induced insulin secretion. *Diabetes Obes. Metab.* 11:168–179. doi:10.1111/j.1463-1326.2009.01109.x

Herchuelz, A., A. Kamagate, H. Ximenes, and F. Van Eylen. 2007. Role of Na/Ca exchange and the plasma membrane Ca^{2+}-ATPase in beta cell function and death. *Ann. NY Acad. Sci.* 1099:456–467. doi:10.1196/annals.1387.048

Herrington, J., M. Sanchez, D. Wunderler, L. Yan, R.M. Bugianesi, I.E. Dick, S.A. Clark, R.M. Brochu, B.T. Priest, M.G. Kohler, and O.B. McManus. 2005. Biophysical and pharmacological properties of the voltage-gated potassium current of human pancreatic beta-cells. *J. Physiol.* 567:159–175. doi:10.1113/jphysiol.2005.089375

Himeno, Y., F. Toyoda, H. Satoh, A. Amano, C.Y. Cha, H. Matsuura, and A. Noma. 2011. Minor contribution of cytosolic Ca^{2+} transients to the pacemaker rhythm in guinea pig sinoatrial node cells. *Am. J. Physiol. Heart Circ. Physiol.* 300:H251–H261. doi:10.1152/ajpheart.00764.2010

Hiriart, M., and D.R. Matteson. 1988. Na channels and two types of Ca channels in rat pancreatic B cells identified with the reverse hemolytic plaque assay. *J. Gen. Physiol.* 91:617–639. doi:10.1085/jgp.91.5.617

Hirschberg, B., J. Maylie, J.P. Adelman, and N.V. Marrion. 1998. Gating of recombinant small-conductance Ca-activated K^+ channels by calcium. *J. Gen. Physiol.* 111:565–581. doi:10.1085/jgp.111.4.565

Hopkins, W.F., S. Fatherazi, B. Peter-Riesch, B.E. Corkey, and D.L. Cook. 1992. Two sites for adenine-nucleotide regulation of ATP-sensitive potassium channels in mouse pancreatic beta-cells and HIT cells. *J. Membr. Biol.* 129:287–295.

Hoth, M., and R. Penner. 1993. Calcium release-activated calcium current in rat mast cells. *J. Physiol.* 465:359–386.

Houamed, K.M., I.R. Sweet, and L.S. Satin. 2010. BK channels mediate a novel ionic mechanism that regulates glucose-dependent electrical activity and insulin secretion in mouse pancreatic β-cells. *J. Physiol.* 588:3511–3523. doi:10.1113/jphysiol.2009.184341

Islam, M.S., O. Larsson, T. Nilsson, and P.O. Berggren. 1995. Effects of caffeine on cytoplasmic free Ca^{2+} concentration in pancreatic beta-cells are mediated by interaction with ATP-sensitive K^+ channels and L-type voltage-gated Ca^{2+} channels but not the ryanodine receptor. *Biochem. J.* 306:679–686.

Jacobson, D.A., F. Mendez, M. Thompson, J. Torres, O. Cochet, and L.H. Philipson. 2010. Calcium-activated and voltage-gated potassium channels of the pancreatic islet impart distinct and complementary roles during secretagogue induced electrical responses. *J. Physiol.* 588:3525–3537. doi:10.1113/jphysiol.2010.190207

Kanno, T., P. Rorsman, and S.O. Göpel. 2002. Glucose-dependent regulation of rhythmic action potential firing in pancreatic beta-cells by K_{ATP}-channel modulation. *J. Physiol.* 545:501–507. doi:10.1113/jphysiol.2002.031344

Keizer, J., and G. Magnus. 1989. ATP-sensitive potassium channel and bursting in the pancreatic beta cell. A theoretical study. *Biophys. J.* 56:229–242. doi:10.1016/S0006-3495(89)82669-4

Kelly, R.P., R. Sutton, and F.M. Ashcroft. 1991. Voltage-activated calcium and potassium currents in human pancreatic beta-cells. *J. Physiol.* 443:175–192.

Kinard, T.A., G. de Vries, A. Sherman, and L.S. Satin. 1999. Modulation of the bursting properties of single mouse pancreatic beta-cells by artificial conductances. *Biophys. J.* 76:1423–1435. doi:10.1016/S0006-3495(99)77303-0

Kukuljan, M., A.A. Goncalves, and I. Atwater. 1991. Charybdotoxin-sensitive $K(_{Ca})$ channel is not involved in glucose-induced electrical activity in pancreatic beta-cells. *J. Membr. Biol.* 119:187–195. doi:10.1007/BF01871418

Larsson, O., H. Kindmark, R. Brandstrom, B. Fredholm, and P.O. Berggren. 1996. Oscillations in K_{ATP} channel activity promote oscillations in cytoplasmic free Ca^{2+} concentration in the pancreatic beta cell. *Proc. Natl. Acad. Sci. USA.* 93:5161–5165. doi:10.1073/pnas.93.10.5161

Leech, C.A., and J.F. Habener. 1998. A role for Ca^{2+}-sensitive nonselective cation channels in regulating the membrane potential of pancreatic beta-cells. *Diabetes.* 47:1066–1073. doi:10.2337/diabetes.47.7.1066

Lytton, J., M. Westlin, S.E. Burk, G.E. Shull, and D.H. MacLennan. 1992. Functional comparisons between isoforms of the sarcoplasmic or endoplasmic reticulum family of calcium pumps. *J. Biol. Chem.* 267:14483–14489.

MacDonald, P.E., A.M. Salapatek, and M.B. Wheeler. 2003. Temperature and redox state dependence of native Kv2.1 currents in rat pancreatic beta-cells. *J. Physiol.* 546:647–653. doi:10.1113/jphysiol.2002.035709

Magnus, G., and J. Keizer. 1998. Model of beta-cell mitochondrial calcium handling and electrical activity. I. Cytoplasmic variables. *Am. J. Physiol.* 274:C1158–C1173.

Marigo, V., K. Courville, W.H. Hsu, J.M. Feng, and H. Cheng. 2009. TRPM4 impacts on Ca^{2+} signals during agonist-induced insulin secretion in pancreatic beta-cells. *Mol. Cell. Endocrinol.* 299:194–203. doi:10.1016/j.mce.2008.11.011

Mears, D., N.F. Sheppard Jr., I. Atwater, E. Rojas, R. Bertram, and A. Sherman. 1997. Evidence that calcium release-activated current mediates the biphasic electrical activity of mouse pancreatic beta-cells. *J. Membr. Biol.* 155:47–59. doi:10.1007/s002329900157

Meissner, H.P., and H. Schmelz. 1974. Membrane potential of beta-cells in pancreatic islets. *Pflugers Arch.* 351:195–206. doi:10.1007/BF00586918

Merrins, M.J., B. Fendler, M. Zhang, A. Sherman, R. Bertram, and L.S. Satin. 2010. Metabolic oscillations in pancreatic islets depend on the intracellular Ca^{2+} level but not Ca^{2+} oscillations. *Biophys. J.* 99:76–84. doi:10.1016/j.bpj.2010.04.012

Meyer-Hermann, M.E. 2007. The electrophysiology of the beta-cell based on single transmembrane protein characteristics. *Biophys. J.* 93:2952–2968. doi:10.1529/biophysj.107.106096

Misler, S., L.C. Falke, K. Gillis, and M.L. McDaniel. 1986. A metabolite-regulated potassium channel in rat pancreatic B cells. *Proc. Natl. Acad. Sci. USA.* 83:7119–7123. doi:10.1073/pnas.83.18.7119

Miura, Y., J.C. Henquin, and P. Gilon. 1997. Emptying of intracellular Ca^{2+} stores stimulates Ca^{2+} entry in mouse pancreatic beta-cells by both direct and indirect mechanisms. *J. Physiol.* 503:387–398. doi:10.1111/j.1469-7793.1997.387bh.x

Miwa, Y., and Y. Imai. 1999. Simulation of spike-burst generation and Ca^{2+} oscillation in pancreatic beta-cells. *Jpn. J. Physiol.* 49:353–364. doi:10.2170/jjphysiol.49.353

Oka, C., C.Y. Cha, and A. Noma. 2010. Characterization of the cardiac Na^+/K^+ pump by development of a comprehensive and mechanistic model. *J. Theor. Biol.* 265:68–77. doi:10.1016/j.jtbi.2010.04.028

Owada, S., O. Larsson, P. Arkhammar, A.I. Katz, A.V. Chibalin, P.O. Berggren, and A.M. Bertorello. 1999. Glucose decreases Na^+,K^+-ATPase activity in pancreatic beta-cells. An effect mediated via Ca^{2+}-independent phospholipase A2 and protein kinase C-dependent phosphorylation of the alpha-subunit. *J. Biol. Chem.* 274:2000–2008. doi:10.1074/jbc.274.4.2000

Plant, T.D. 1988. Properties and calcium-dependent inactivation of calcium currents in cultured mouse pancreatic B-cells. *J. Physiol.* 404:731–747.

Prakriya, M., and R.S. Lewis. 2002. Separation and characterization of currents through store-operated CRAC channels and Mg^{2+}-inhibited cation (MIC) channels. *J. Gen. Physiol.* 119:487–507. doi:10.1085/jgp.20028551

Ribalet, B., and P.M. Beigelman. 1980. Calcium action potentials and potassium permeability activation in pancreatic beta-cells. *Am. J. Physiol.* 239:C124–C133.

Roe, M.W., L.H. Philipson, C.J. Frangakis, A. Kuznetsov, R.J. Mertz, M.E. Lancaster, B. Spencer, J.F. Worley III, and I.D. Dukes. 1994.

Defective glucose-dependent endoplasmic reticulum Ca^{2+} sequestration in diabetic mouse islets of Langerhans. *J. Biol. Chem.* 269:18279–18282.

Rorsman, P., and G. Trube. 1985. Glucose dependent K^+-channels in pancreatic beta-cells are regulated by intracellular ATP. *Pflugers Arch.* 405:305–309. doi:10.1007/BF00595682

Rorsman, P., and G. Trube. 1986. Calcium and delayed potassium currents in mouse pancreatic beta-cells under voltage-clamp conditions. *J. Physiol.* 374:531–550.

Rorsman, P., H. Abrahamsson, E. Gylfe, and B. Hellman. 1984. Dual effects of glucose on the cytosolic Ca^{2+} activity of mouse pancreatic beta-cells. *FEBS Lett.* 170:196–200. doi:10.1016/0014-5793(84)81398-8

Rorsman, P., P. Arkhammar, and P.O. Berggren. 1986. Voltage-activated Na^+ currents and their suppression by phorbol ester in clonal insulin-producing RINm5F cells. *Am. J. Physiol.* 251:C912–C919.

Rorsman, P., C. Ämmälä, P.O. Berggren, K. Bokvist, and O. Larsson. 1992. Cytoplasmic calcium transients due to single action potentials and voltage-clamp depolarizations in mouse pancreatic B-cells. *EMBO J.* 11:2877–2884.

Santos, R.M., and E. Rojas. 1989. Muscarinic receptor modulation of glucose-induced electrical activity in mouse pancreatic B-cells. *FEBS Lett.* 249:411–417. doi:10.1016/0014-5793(89)80669-6

Santos, R.M., L.M. Rosario, A. Nadal, J. Garcia-Sancho, B. Soria, and M. Valdeolmillos. 1991. Widespread synchronous $[Ca^{2+}]_i$ oscillations due to bursting electrical activity in single pancreatic islets. *Pflugers Arch.* 418:417–422. doi:10.1007/BF00550880

Satin, L.S., and D.L. Cook. 1989. Calcium current inactivation in insulin-secreting cells is mediated by calcium influx and membrane depolarization. *Pflugers Arch.* 414:1–10. doi:10.1007/BF00585619

Satin, L.S., W.F. Hopkins, S. Fatherazi, and D.L. Cook. 1989. Expression of a rapid, low-voltage threshold K current in insulin-secreting cells is dependent on intracellular calcium buffering. *J. Membr. Biol.* 112:213–222. doi:10.1007/BF01870952

Schulla, V., E. Renström, R. Feil, S. Feil, I. Franklin, A. Gjinovci, X.J. Jing, D. Laux, I. Lundquist, M.A. Magnuson, et al. 2003. Impaired insulin secretion and glucose tolerance in beta cell-selective $Ca_v1.2$ Ca^{2+} channel null mice. *EMBO J.* 22:3844–3854. doi:10.1093/emboj/cdg389

Sherman, A., J. Rinzel, and J. Keizer. 1988. Emergence of organized bursting in clusters of pancreatic beta-cells by channel sharing. *Biophys. J.* 54:411–425. doi:10.1016/S0006-3495(88)82975-8

Sherman, A., J. Keizer, and J. Rinzel. 1990. Domain model for Ca^{2+}-inactivation of Ca^{2+} channels at low channel density. *Biophys. J.* 58:985–995. doi:10.1016/S0006-3495(90)82443-7

Smith, P.A., P. Rorsman, and F.M. Ashcroft. 1989. Modulation of dihydropyridine-sensitive Ca^{2+} channels by glucose metabolism in mouse pancreatic beta-cells. *Nature.* 342:550–553. doi:10.1038/342550a0

Smith, P.A., F.M. Ashcroft, and P. Rorsman. 1990a. Simultaneous recordings of glucose dependent electrical activity and ATP-regulated K^+-currents in isolated mouse pancreatic beta-cells. *FEBS Lett.* 261:187–190. doi:10.1016/0014-5793(90)80667-8

Smith, P.A., K. Bokvist, P. Arkhammar, P.O. Berggren, and P. Rorsman. 1990b. Delayed rectifying and calcium-activated K^+ channels and their significance for action potential repolarization in mouse pancreatic β-cells. *J. Gen. Physiol.* 95:1041–1059. doi:10.1085/jgp.95.6.1041

Smolen, P. 1995. A model for glycolytic oscillations based on skeletal muscle phosphofructokinase kinetics. *J. Theor. Biol.* 174:137–148. doi:10.1006/jtbi.1995.0087

Smolen, P., and J. Keizer. 1992. Slow voltage inactivation of Ca^{2+} currents and bursting mechanisms for the mouse pancreatic beta-cell. *J. Membr. Biol.* 127:9–19.

Sturgess, N.C., C.N. Hales, and M.L. Ashford. 1987. Calcium and ATP regulate the activity of a non-selective cation channel in a rat insulinoma cell line. *Pflugers Arch.* 409:607–615. doi:10.1007/BF00584661

Takeuchi, A., S. Tatsumi, N. Sarai, K. Terashima, S. Matsuoka, and A. Noma. 2006. Ionic mechanisms of cardiac cell swelling induced by blocking Na^+/K^+ pump as revealed by experiments and simulation. *J. Gen. Physiol.* 128:495–507. doi:10.1085/jgp.200609646

Tamarina, N.A., Y. Wang, L. Mariotto, A. Kuznetsov, C. Bond, J. Adelman, and L.H. Philipson. 2003. Small-conductance calcium-activated K^+ channels are expressed in pancreatic islets and regulate glucose responses. *Diabetes.* 52:2000–2006. doi:10.2337/diabetes.52.8.2000

Tengholm, A., B. Hellman, and E. Gylfe. 2001. The endoplasmic reticulum is a glucose-modulated high-affinity sink for Ca^{2+} in mouse pancreatic beta-cells. *J. Physiol.* 530:533–540. doi:10.1111/j.1469-7793.2001.0533k.x

Tse, F.W., A. Tse, and B. Hille. 1994. Cyclic Ca^{2+} changes in intracellular stores of gonadotropes during gonadotropin-releasing hormone-stimulated Ca^{2+} oscillations. *Proc. Natl. Acad. Sci. USA.* 91:9750–9754. doi:10.1073/pnas.91.21.9750

Váradi, A., E. Molnár, and S.J. Ashcroft. 1995. Characterisation of endoplasmic reticulum and plasma membrane Ca^{2+}-ATPases in pancreatic beta-cells and in islets of Langerhans. *Biochim. Biophys. Acta.* 1236:119–127. doi:10.1016/0005-2736(95)00103-A

Váradi, A., E. Molnár, C.G. Ostenson, and S.J. Ashcroft. 1996. Isoforms of endoplasmic reticulum Ca^{2+}-ATPase are differentially expressed in normal and diabetic islets of Langerhans. *Biochem. J.* 319:521–527.

Velasco, J.M., and O.H. Petersen. 1987. Voltage-activation of high-conductance K^+ channel in the insulin-secreting cell line RINm5F is dependent on local extracellular Ca2+ concentration. *Biochim. Biophys. Acta.* 896:305–310. doi:10.1016/0005-2736(87)90191-X

Vignali, S., V. Leiss, R. Karl, F. Hofmann, and A. Welling. 2006. Characterization of voltage-dependent sodium and calcium channels in mouse pancreatic A- and B-cells. *J. Physiol.* 572:691–706.

Worley, J.F., III, M.S. McIntyre, B. Spencer, and I.D. Dukes. 1994a. Depletion of intracellular Ca^{2+} stores activates a maitotoxin-sensitive nonselective cationic current in beta-cells. *J. Biol. Chem.* 269:32055–32058.

Worley, J.F., III, M.S. McIntyre, B. Spencer, R.J. Mertz, M.W. Roe, and I.D. Dukes. 1994b. Endoplasmic reticulum calcium store regulates membrane potential in mouse islet beta-cells. *J. Biol. Chem.* 269:14359–14362.

Zhang, M., P. Goforth, R. Bertram, A. Sherman, and L. Satin. 2003. The Ca^{2+} dynamics of isolated mouse beta-cells and islets: implications for mathematical models. *Biophys. J.* 84:2852–2870. doi:10.1016/S0006-3495(03)70014-9

Zhang, M., K. Houamed, S. Kupershmidt, D. Roden, and L.S. Satin. 2005. Pharmacological properties and functional role of K_{slow} current in mouse pancreatic β-cells: SK channels contribute to K_{slow} tail current and modulate insulin secretion. *J. Gen. Physiol.* 126:353–363. doi:10.1085/jgp.200509312

BJ www.biochemj.org

Biochem. J. (2011) 435, 421–430 (Printed in Great Britain) doi:10.1042/BJ20101708

Role of mitochondrial phosphate carrier in metabolism–secretion coupling in rat insulinoma cell line INS-1

Yuichi NISHI, Shimpei FUJIMOTO[1], Mayumi SASAKI, Eri MUKAI, Hiroki SATO, Yuichi SATO, Yumiko TAHARA, Yasuhiko NAKAMURA and Nobuya INAGAKI

Department of Diabetes and Clinical Nutrition, Graduate School of Medicine, Kyoto University, 54 Shogoin Kawahara-cho, Sakyo-ku, Kyoto 606–8507, Japan

In pancreatic β-cells, glucose-induced mitochondrial ATP production plays an important role in insulin secretion. The mitochondrial phosphate carrier PiC is a member of the SLC25 (solute carrier family 25) family and transports P_i from the cytosol into the mitochondrial matrix. Since intramitochondrial P_i is an essential substrate for mitochondrial ATP production by complex V (ATP synthase) and affects the activity of the respiratory chain, P_i transport via PiC may be a rate-limiting step for ATP production. We evaluated the role of PiC in metabolism–secretion coupling in pancreatic β-cells using INS-1 cells manipulated to reduce PiC expression by siRNA (small interfering RNA). Consequent reduction of the PiC protein level decreased glucose (10 mM)-stimulated insulin secretion, the ATP:ADP ratio in the presence of 10 mM glucose and elevation of intracellular calcium concentration in response to 10 mM glucose without affecting the mitochondrial membrane potential ($\Delta\psi_m$) in INS-1 cells. In experiments using the mitochondrial fraction of INS-1 cells in the presence of 1 mM succinate, PiC down-regulation decreased ATP production at various P_i concentrations ranging from 0.001 to 10 mM, but did not affect $\Delta\psi_m$ at 3 mM P_i. In conclusion, the P_i supply to mitochondria via PiC plays a critical role in ATP production and metabolism–secretion coupling in INS-1 cells.

Key words: inorganic phosphate (P_i), insulin secretion, mitochondria, mitochondrial phosphate carrier (PiC), small interfering RNA (siRNA), solute carrier family 25 (SLC25).

INTRODUCTION

Glucose stimulates insulin secretion by both triggering and amplifying signals in pancreatic β-cells [1]. The triggering pathway includes entry of glucose into β-cells, acceleration of glycolysis in the cytosol and mitochondrial metabolism of products derived from glycolysis, increase in ATP content and ATP/ADP ratio, closure of ATP-sensitive K^+ channels (K_{ATP} channels), membrane depolarization, opening of VDCCs (voltage-dependent Ca^{2+} channels), increase in Ca^{2+} influx through VDCCs, rise in intracellular Ca^{2+} concentration ($[Ca^{2+}]_i$), and exocytosis of insulin granules. Glucose also exerts its effects by increasing Ca^{2+} efficacy in stimulation–secretion coupling via an amplifying pathway, owing at least in part to the direct effect of increased ATP derived from glucose metabolism on exocytosis. Since depletion of mitochondrial DNA abolishes the glucose-induced ATP elevation, mitochondria are clearly a major source of ATP production in pancreatic β-cells [2,3]. Collectively, in pancreatic β-cells, intracellular glucose metabolism regulates exocytosis of insulin granules according to metabolism–secretion coupling in which glucose-induced mitochondrial ATP production plays an important role.

Almost all of the mitochondrial carrier proteins are embedded in the inner membranes of mitochondria, where they transport solutes across the membrane. They belong to the SLC25 (solute carrier family 25) group of proteins [4]. Several members of the SLC25 group have been reported to play roles in GSIS (glucose-stimulated insulin secretion) in pancreatic β-cells. Overexpression or silencing of AGC1 (aspartate/glutamate carrier 1; SLC25A12 or Aralar1) has been reported to increase or reduce GSIS in INS-1E cells respectively [5,6]. Overexpression of UCP2 (uncoupling protein 2; SLC25A8) by adenovirus vector is known to inhibit GSIS from rat islets [7], whereas GSIS from islets of UCP2-deficient mice is enhanced compared with that from control islets [8]. In addition, down-regulation of OGC (2-oxoglutarate carrier; SLC25A11), CIC (citrate/isocitrate carrier; SLC25A1) and GC1 (glutamate carrier 1; SLC25A22) by siRNA (small interfering RNA) suppress GSIS [9–11].

The mitochondrial phosphate carrier PiC (SLC25A3) is a member of the SLC25 family and transports P_i from the cytosol into the mitochondrial matrix. The *PiC* gene has 9 exons; the 3rd and the 4th exons are called exon 3A and exon 3B respectively. These two exons are alternatively spliced and two isoforms of PiC, PiC-A and PiC-B, are generated [12]. They differ considerably in their kinetic parameters as previously shown in a study using a reconstitution system [13]. The K_m of PiC-A for P_i on the external membrane surface is 3-fold that of PiC-B (PiC-A: ~2.2 mM; PiC-B: ~0.78 mM). The K_m on the internal surface is much higher (PiC-A: ~9.7 mM; PiC-B: ~6.3 mM) than K_m on the external membrane surface. The maximum transport rate of PiC-A is approximately a third that of PiC-B. These isoforms also differ in their tissue distribution. PiC-A is expressed in skeletal muscle and cardiac muscle, whereas PiC-B is expressed ubiquitously [13,14]. A case study of patients with PiC-A deficiency who suffered from lactic acidosis, heart failure and muscle weakness and died within the first year of life, demonstrates the critical significance of this carrier [15].

Since intramitochondrial P_i is an essential substrate for mitochondrial ATP production by complex V (ATP synthase) and affects activity of the respiratory chain [16], the supply of P_i from

Abbreviations used: AAC, ATP/ADP carrier; DAPP, diadenosine pentaphosphate; DIC, dicarboxylate carrier; FCCP, carbonyl cyanide *p*-trifluoromethoxyphenylhydrazone; GSIS, glucose-stimulated insulin secretion; KRBH, Krebs-Ringer bicarbonate Hepes buffer; RT, reverse transcription; siRNA, small interfering RNA; SLC25, solute carrier family 25; TMPD, *N*,*N*,*N*′,*N*′-tetramethyl-*p*-phenylenediamine.

[1] To whom correspondence should be addressed (email fujimoto@metab.kuhp.kyoto-u.ac.jp).

cytosol to mitochondrial matrix via PiC may be a rate-limiting step for ATP production. However, precise detection of PiC and its significance in metabolism–secretion coupling in pancreatic β-cells has not been reported previously. In the present study, the role of PiC in metabolism–secretion coupling in pancreatic β-cells is evaluated using INS-1 cells manipulated to reduce PiC expression.

EXPERIMENTAL

Materials

ATP, ADP, poly-L-ornithine, DAPP (diadenosine pentaphosphate), Safranin O, FCCP (carbonyl cyanide *p*-trifluoromethoxyphenylhydrazone), ATP sulfurylase and Na_2MoO_4 were purchased from Sigma. Hepes, KCl, EGTA, sodium pyruvate, $MgSO_4$, NaH_2PO_4, $CaCl_2$, glucose, NaCl, $NaHCO_3$, $HClO_4$, Na_2CO_3, pyruvate kinase, BSA, KOH, potassium gluconate and KH_2PO_4 were purchased from Nacalai. 2-mercaptoethanol, penicillin, streptomycin and mouse monoclonal antibodies to the subunits of the mitochondrial respiratory chain complexes were purchased from Invitrogen. Luciferin-luciferase was purchased from Promega.

Cell culture

INS-1 (rat insulinoma) cells were cultured in RPMI 1640 medium containing 11.1 mM glucose (Invitrogen) supplemented with 10 % heat-inactivated fetal calf serum, 10 mM Hepes, 2 mM L-glutamine, 1 mM sodium pyruvate, 50 μM 2-mercaptoethanol, 100 IU/ml penicillin and 100 μg/ml streptomycin at 37 °C in a humidified atmosphere (5 % CO_2 and 95 % air). COS-7 (African green monkey kidney) cells were cultured in Dulbecco's modified Eagle's medium supplemented with 10 % heat-inactivated fetal calf serum, 100 IU/ml penicillin and 100 μg/ml streptomycin at 37 °C in a humidified atmosphere (5 % CO_2 and 95 % air).

siRNA transfection

Stealth™ siRNAs were synthesized by Invitrogen. The sequences of siRNAs specific for both rat PiC-A and PiC-B were: 5′-AAAUAUGCCCUUGUACUUCUGAGGG-3′ and 5′-CCCUCAGAAGUACAAGGGCAUAUUU-3′ designated as PiC siRNA1 and 5′-GAACACCUAUCUGUGGCGUACAUCA-3′ and 5′-UGAUGUACGCCACAGAUAGGUGUUC-3′ designated as PiC siRNA2. The sequences of control siRNAs were: 5′-ACCAACAACAGUUUGGGAAUAGGGA-3′ and 5′-UCCCUAUUCCCAAACUGUUGUUGGU-3′. Cultured INS-1 cells were trypsinized, suspended with RPMI 1640 medium without antibiotics, mixed with Opti-MEM (Invitrogen) containing siRNA and Lipofectamine™ 2000 (Invitrogen), plated on dishes or wells and then incubated at 37 °C in a CO_2 incubator. The final amounts of INS-1 cells, RPMI 1640, Opti-MEM, siRNA and Lipofectamine™ 2000 were 1×10^6 cells/ml, 75 % (v/v), 25 % (v/v), 80 nM and 0.3 % respectively. Medium was replaced with RPMI 1640 3–4 h after transfection. All experiments using siRNA-transfected INS-1 cells were performed 48 h after transfection unless otherwise noted.

Isolation of total RNA and quantitative RT (reverse transcription)–PCR

Total RNA was isolated from cardiac muscle, brain, skeletal muscle, kidney, liver and lung of Wistar rats using TRIzol® (Invitrogen) and from islets of Wistar rats and INS-1 cells using RNeasy mini kit (Qiagen). Animals were maintained and used in accordance with the Guidelines for Animal Experiments of Kyoto University. Islets were isolated by collagenase digestion [17]. cDNA was prepared by reverse transcriptase (Superscript II; Invitrogen) with an oligo(dT) primer. The rat sequences of forward and reverse primers to detect PiC-A, PiC-B, total PiC (PiC-A plus PiC-B) and β-actin (as an inner control) are shown in Table 1. AmpliTaq Gold (Applied Biosystems) was used as a DNA polymerase for RT–PCR. SYBR Green PCR Master Mix (Applied Biosystems) was prepared for the quantitative RT–PCR run. The thermal cycling conditions were denaturation at 95 °C for 10 min followed by 40 cycles at 95 °C for 30s and 60 °C for 30s.

Table 1 Primer sequences used in RT–PCR and quantitative RT–PCR

Name	Forward	Reverse
PiC-A	5′-AGCTGGTGCACGATGTGTCG-3′	5′-TTCCTCCGAGTCCACAGAGG-3′
PiC-B	5′-AGCTGGTGCACGATGTGTCG-3′	5′-CCACCAAAGCCACACAGTGC-3′
Total PiC (PiC-A+PiC-B)	5′-AGAGCAGCTGGTTGTGACAT-3′	5′-ACACCTCTAAAGCCAAGCCT-3′
β-actin	5′-CAATGAGCGGTTCCGATGCC-3′	5′-AATGCCTGGGTACATGGTGG-3′

Plasmid construction and transfection

The cDNA fragment of rat PiC-B was obtained from rat islets by RT–PCR and cloned into the pHMCA5 vector. pHMCA5-PiC-B was transfected into COS-7 and INS-1 cells using FuGENE™ 6 transfection reagent (Roche) and Lipofectamine™ 2000 respectively.

Immunoblot analysis

Rabbit antibody against the rat PiC peptide PPEM-PESLKKKLGLTE corresponding to C-terminal residues was originally raised. For immunoblotting, cells were washed with PBS containing protease inhibitor (Complete; Roche), suspended in 1 ml of PBS containing protease inhibitor and homogenized. Protein (50 μg per sample) was separated on a 15 % polyacrylamide gel and transferred to a nitrocellulose membrane. After blocking with TBS (Tris-buffered saline; 10 mM Tris/HCl and 100 mM NaCl, pH 7.5) containing 0.1 % Tween 20 and 5 % skimmed milk (blocking buffer) at room temperature (25 °C) for 2 h, blotted membranes were incubated overnight at 4 °C with anti-PiC antibody at 1:500 dilution, anti-DIC (dicarboxylate carrier) antibody (Novus Biologicals) at 1:100 dilution, mouse monoclonal anti-complex I (39 kDa subunit) antibody, anti-complex III (core II) antibody, anti-complex IV (subunit I) antibody or anti-complex V (subunit α) of mitochondrial respiratory chain antibody at 1:1000 dilution in blocking buffer, and subsequently with anti-rabbit (for PiC and DIC) or anti-mouse (for respiratory chain proteins) IgG horseradish peroxidase-conjugated secondary antibody (GE Healthcare) diluted 1:5000 at room temperature for 2 h prior to detection using ECL (GE Healthcare). In the same membrane, the process was repeated for β-actin at 1:1000 dilution of the antibody. Band intensities were quantified with Multi Gauge software (Fujifilm).

Insulin secretion

For insulin secretion assays, INS-1 cells cultured on 24-well plates coated with 0.001 % poly-L-ornithine were washed with KRBH (Krebs-Ringer bicarbonate Hepes buffer) composed of

140 mM NaCl, 3.6 mM KCl, 0.5 mM $MgSO_4$, 0.5 mM NaH_2PO_4, 1.5 mM $CaCl_2$, 2 mM $NaHCO_3$, 0.1 % BSA and 10 mM Hepes (pH 7.4) with 2 mM glucose, preincubated at 37 °C for 30 min in KRBH with 2 mM glucose, and then incubated at 37 °C for 30 min in KRBH with 2 mM glucose, 10 mM glucose or 2 mM glucose plus 30 mM KCl. Insulin concentrations were determined by RIA using rat insulin as a standard as previously described [17].

Adenine nucleotides

ATP and ADP contents were determined as previously described [18,19] with some modifications. Briefly, INS-1 cells were cultured, washed and preincubated as described above and incubated with KRBH with 2 mM glucose, 10 mM glucose or 2 mM glucose plus 30 mM KCl at 37 °C for 30 min. Incubation was stopped by the addition of $HClO_4$. The contents of wells were sonicated [three pulses of 3 s duration using a Handy Sonic UR-20P instrument (TOMY SEIKO) on ice] and transferred into glass tubes. The tubes were then centrifuged, and a fraction of the supernatant was neutralized with Hepes and Na_2CO_3. The ATP concentration was measured by luciferin-luciferase assay. After ATP in the neutralized extract was irreversibly converted to AMP with ATP sulfurylase in the presence of Na_2MoO_4, ADP in the reactant was converted to ATP with pyruvate kinase and was determined by luciferin-luciferase assay as the difference between the measurements with and without pyruvate kinase.

Intracellular calcium concentration ($[Ca^{2+}]_i$) and mitochondrial membrane potential ($\Delta\psi_m$) in living cells

INS-1 cells were seeded on to glass coverslips coated with 0.001 % poly-L-ornithine and cultured 48 h before measurements were made. For measurements of $[Ca^{2+}]_i$, cultured INS-1 cells were loaded with 5 μM Fura-PE3/AM (Calbiochem) at 37 °C for 90 min, placed in a heat-controlled chamber on the stage of an inverted microscope kept at 36 ± 1 °C, superfused with KRBH containing 2 mM glucose, and subsequently exposed to the buffer containing 10 mM glucose or 30 mM KCl. The cells were excited successively at 340 and 380 nm, and the fluorescence emitted at 510 nm was captured by CCD camera (Micro Max 5 MHz System, Roper Industries, Trenton, NJ). The images were analysed with the Meta Fluor image analyzing system (Universal Imaging). The 340 nm (F340) and 380 nm (F380) fluorescence signals were detected every 15 s, and ratios (F340/F380) were calculated. For $\Delta\psi_m$ measurements, the same protocol as above was used except that cultured cells were loaded with 10 μg/ml rhodamine 123 (Invitrogen) at 37 °C for 30 min and fluorescence excited at 490 nm and emitted at 530 nm every 20 s was monitored.

ATP production and $\Delta\psi_m$ in mitochondrial fraction

Measurement of ATP production from the mitochondrial fraction was performed as previously described [18] with minor modifications. Firstly, INS-1 cells were homogenized in solution A consisting of 50 mM Hepes, 100 mM KCl, 1.8 mM ATP, 1 mM EGTA, 2 mM $MgCl_2$ and 0.5 mg/ml BSA (electrophoretically homogeneous) with the pH adjusted to 7.00 at 37 °C with KOH. After precipitation of cell debris and nuclei by 800 *g* centrifugation for 3 min, the supernatant was centrifuged more rapidly (10000 *g* for 3 min) to obtain a pellet containing the mitochondrial fraction. The precipitation, diluted by 200 μl of solution A, was centrifuged again and rinsed three times in solution B, consisting of 20 mM Hepes, 1 mM EGTA, 12 mM NaCl, 0.3 mM $MgCl_2$, 130 mM potassium gluconate and 0.5 mg/ml BSA (electrophoretically homogeneous) with the pH adjusted to 7.10 with KOH. The mitochondrial fraction in 500 μl of solution B was kept on ice until use. To measure ATP production by oxidative phosphorylation, the reaction was started by adding mitochondrial suspension to prewarmed solution B (37 °C) containing mitochondrial substrates with or without respiratory chain inhibitors, 50 μM ADP, 1 μM DAPP and various levels of P_i. DAPP, a specific inhibitor of adenylate kinase, was used to measure ATP production by oxidative phosphorylation exclusively. After the reaction was stopped, the ATP concentration in the solutions was measured by adding luciferin-luciferase solution with a bioluminometer. ATP production was corrected by mitochondrial protein content. Measurement of $\Delta\psi_m$ was performed as previously described [20] with some modifications. Fluorescence was successively monitored using a spectrofluorophotometer (RF 5000; Shimadzu) with an excitation wavelength of 495 nm and emission at 586 nm, and with stirring solution B supplemented with 3 mM KH_2PO_4, 50 μM ADP and 2.5 μM Safranin O applied in a glass cuvette at 37 °C. Mitochondria, succinate and FCCP were added to the solution in this order and final concentrations were 50 μg/ml, 1 mM and 200 nM respectively.

Statistical analysis

The data are expressed as means ± S.E.M. Statistical significance was calculated by unpaired Student's *t* test. $P < 0.05$ was considered significant.

RESULTS

Expression of PiC mRNA in pancreatic β-cells

Tissue distribution of PiC was evaluated by RT–PCR (Figure 1A). PiC-B was expressed ubiquitously whereas PiC-A was expressed clearly in cardiac muscle and skeletal muscle as previously reported [13,14] and obscurely in rat islets and INS-1 cells. These results indicate that PiC-B was dominantly expressed in pancreatic β-cells.

Evaluation of anti-PiC antibody

The cell lysates of COS-7 cells transfected with pHMCA5-PiC or pHMCA5-null, INS-1 cells transfected with pHMCA5-null, intact INS-1 cells and rat islets were electrophoresed and immunoblotted using the anti-PiC antibody. As shown in Figure 1(B), the band at ~30 kDa, which was not detected in COS-7 cells transfected with pHMCA5-null, was detected in COS-7 cells transfected with pHMCA5-PiC, INS-1 cells transfected with pHMCA5-null, intact INS-1 cells and rat islets. This observation is consistent with a previous report that rat PiC was detected at ~30 kDa by an antibody originally raised using the C-terminal amino acids as the antigen peptide [21].

Silencing effects of PiC siRNAs on INS-1 cells

Quantitative RT–PCR assays using primers for total PiC (PiC-A plus PiC-B, Table 1) and immunoblotting using anti-PiC antibody revealed ~70 % reduction of PiC mRNA expression and ~40 % reduction of the protein expression in INS-1 cells 48 h after both PiC siRNA1 and 2 transfection respectively (Figures 1C and 1D). Time-dependent reduction of PiC protein expression (~25 %, ~40 % and ~50 % reduction at 24 h, 48 h and 72 h after siRNA1 and 2 transfection) implies long half-life of PiC, which causes low efficacy of suppression (Figure 1D). Transfection of control siRNA did not affect the expression of PiC in INS-1 cells at both mRNA and protein levels. Protein expressions of DIC,

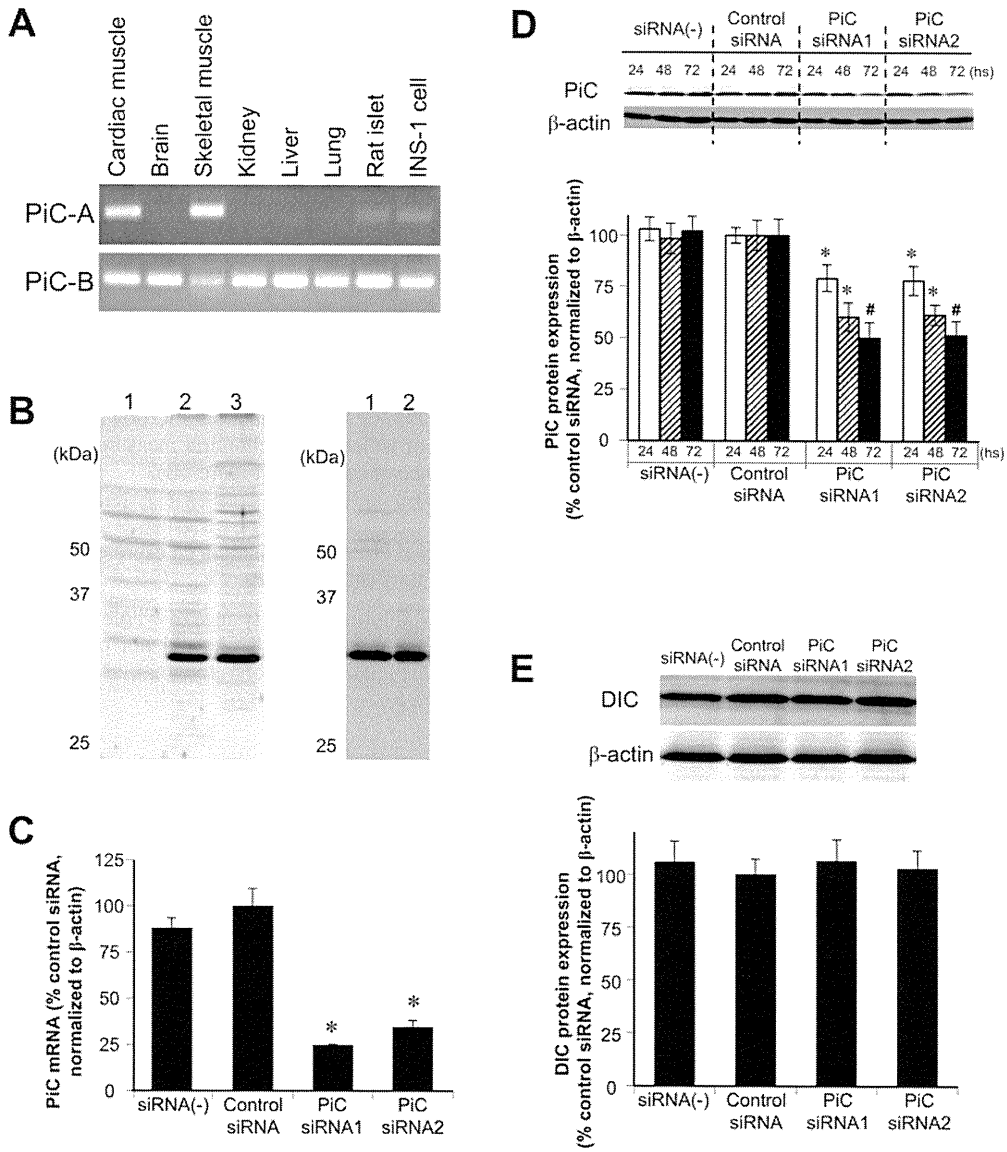

Figure 1 Detection of rat PiC and silencing effects of PiC siRNAs on INS-1 cells

(**A**) RT–PCR detection of PiC mRNA expression in various rat tissues and INS-1 cells. PiC mRNA expressions in cardiac muscle, brain, skeletal muscle, kidney, liver, lung and islets of Wistar rat and INS-1 cells were evaluated with RT–PCR using primers of specific sequences for PiC-A and PiC-B. Product sizes are 141 bp for PiC-A and 136 bp for PiC-B. (**B**) Evaluation of anti-PiC antibody by immunoblot analysis. Left panel: whole cell lysates from COS-7 cells transfected with pHMCA5-null (lane 1), COS-7 cells transfected with pHMCA5-PiC (lane 2) and INS-1 cells transfected with pHMCA5-null (lane 3) were electrophoresed and immunoblotted with anti-PiC antibody. Right panel: whole cell lysates from INS-1 cells (lane 1) and rat islets (lane 2) were electrophoresed and immunoblotted with anti-PiC antibody. Molecular mass in kDa is given on the left-hand side of each panel. (**C**) Effects of transfection of PiC siRNAs on the expression of PiC mRNA was evaluated with quantitative RT–PCR using a pair of primers recognizing both PiC-A and PiC-B (total PiC). Data were normalized using β-actin mRNA. $n = 3$ in each group. $^*P < 0.01$ compared with control siRNA. (**D**) Immunoblot analysis of PiC expression revealed that PiC siRNAs reduced PiC expression in INS-1 cells. Time (h) after siRNA transfection is indicated. Data were normalized by the expression of β-actin. $n = 4$ in each bar. $^*P < 0.05$ and $\#P < 0.01$ compared with control siRNA. (**E**) Effects of PiC silencing on expression of DIC. Whole INS-1 cell lysate was electrophoresed and immunoblotted using antibodies against DIC. Quantification data were obtained from four independent experiments and normalized with β-actin levels.

another P_i carrier, were not affected by siRNA1 and 2 transfection (Figure 1E).

Effects of PiC down-regulation on glucose- and depolarization-stimulated insulin secretion

Down-regulation of PiC decreased GSIS (10 mM glucose) in INS-1 cells, as shown in Figure 2. A reduction in GSIS of 61 % by PiC siRNA1 and 47 % by PiC siRNA2 was observed. K^+ (30 mM)-stimulated insulin secretion was also reduced: the reduction was 27 % by PiC siRNA1 and 23 % by PiC siRNA2, which were milder than those of GSIS (Figure 2). Insulin secretion in the basal glucose state (2 mM) was not affected by PiC siRNA1, but was slightly increased by PiC siRNA2. Transfection of control siRNA did not affect GSIS in INS-1 cells.

Effects of PiC down-regulation on adenine nucleotides

Down-regulation of PiC increased ADP and decreased the ATP:ADP ratio, whereas it did not significantly affect ATP in

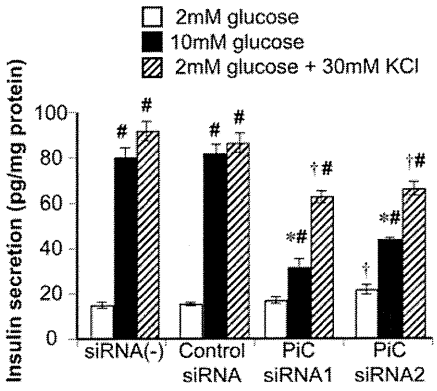

Figure 2 Effects of PiC down-regulation on glucose- or KCl-stimulated insulin secretion

INS-1 cells were incubated for 30 min with 2 mM glucose, 10 mM glucose or 2 mM glucose and 30 mM K^+, and insulin secretion was measured. Data were obtained from six independent experiments normalized by protein concentration. Error bars are means ± S.E.M. *$P < 0.01$ and †$P < 0.05$ compared with control siRNA at the corresponding condition. #$P < 0.01$ compared with corresponding 2 mM glucose.

the presence of 10 mM glucose in INS-1 cells (Table 2A). ATP, ADP and the ATP:ADP ratio at 2 mM glucose was not altered by silencing PiC (Tables 2A and 2B). Depolarization evoked by 30 mM K^+ in the presence of 2 mM glucose decreased the ATP:ADP ratio in both control and PiC down-regulated cells, whereas suppression of the ATP:ADP ratio was lower in PiC down-regulated cells compared with control cells (Table 2B).

Effects of PiC down-regulation on $[Ca^{2+}]_i$ and $\Delta\psi_m$ in living cells

Fluorescence signals of Fura-PE3 revealed that elevation of $[Ca^{2+}]_i$ in response to a stimulating level of 10 mM glucose was decreased and delayed by PiC down-regulation compared with that in control (Figure 3A). Average values calculated using the data from Figure 3(A) also indicate that PiC siRNA reduced the mean $[Ca^{2+}]_i$ at 10 mM glucose (PiC siRNA1, 0.864 ± 0.004 compared with control siRNA, 0.896 ± 0.003; $P < 0.01$) whereas there was no significant change at basal (2 mM) glucose (PiC siRNA1, 0.846 ± 0.004; control siRNA, 0.857 ± 0.003), as shown in Figure 3(B). Elevation of $[Ca^{2+}]_i$ in response to 30 mM K^+ was slightly decreased by PiC siRNA1 (average value of Fura-PE3 fluorescence ratio was 0.968 ± 0.005, compared with a control siRNA ratio of 0.991 ± 0.005, $P < 0.01$) without affecting basal value (control siRNA, 0.857 ± 0.006; siRNA1, 0.854 ± 0.004) as shown in Figures 3(C) and 3(D). Fluorescence measurement using rhodamine 123 demonstrated that the mitochondrial membrane in INS-1 cells was hyperpolarized by raising glucose from 2 to 10 mM and prominently depolarized by FCCP, and that PiC down-regulation did not affect glucose-induced hyperpolarization and total depolarization after FCCP exposure of $\Delta\psi_m$ throughout the measurement (Figure 3E).

Effects of PiC down-regulation on ATP production and $\Delta\psi_m$ in mitochondrial fraction

ATP production by mitochondria from INS-1 cells transfected with control or PiC siRNAs in the presence of 1 mM succinate and various concentrations of P_i ($[P_i]$) is shown in Figure 4(A). PiC down-regulation decreased mitochondrial ATP production by 50–60 % at $[P_i]$ ranging from 0.001 to 10 mM. ATP production in all groups reached maximum rates above ~3 mM of $[P_i]$, which indicates that the PiC amount regulates the maximal rate of mitochondrial ATP production. On the other hand, K_m values of $[P_i]$ for ATP production were similar (~0.05 mM). Mitochondrial ATP production in the presence of various mitochondrial substrates and inhibitors of the respiratory chain is shown in Table 3. ATP production in the presence of succinate was completely inhibited by antimycin A, a complex III inhibitor, in both control and PiC down-regulated INS-1 cells. PiC siRNAs decreased ATP production in the presence of pyruvate and malate by 42–58 %, succinate plus rotenone by 46–62 % and TMPD (*N*,*N*,*N*′,*N*′-tetramethyl-*p*-phenylenediamine) plus ascorbate by 61–62 %, showing that ATP production by electrons rendered at complex I, complex II and complex IV is suppressed to a similar degree. In spite of significant down-regulation of ATP production, PiC down-regulation did not affect $\Delta\psi_m$ of isolated mitochondria measured with Safranin O in the presence of succinate (Figure 4B).

Effects of PiC down-regulation on expression of mitochondrial respiratory chain proteins

Immunoblotting using lysates of whole INS-1 cells revealed that transfection of PiC siRNAs did not change the expression of complex I, III, IV or V of mitochondrial respiratory chain proteins (Figure 5).

DISCUSSION

In the present study, the mitochondrial phosphate carrier (PiC) was revealed to play an important role in metabolism–secretion coupling of pancreatic β-cells by using INS-1 cells and PiC siRNA. PiC down-regulation brings about reduction in mitochondrial ATP production by mitochondrial fuels, resulting in reduced glucose-induced $[Ca^{2+}]_i$ elevation and impaired GSIS.

In pancreatic β-cells, ATP increase is slight and ADP decrease is prominent via an increase in glucose levels beyond the triggering level of insulin secretion. In addition, the ATP/ADP ratio is well-correlated with GSIS rather than the absolute value of ATP [22,23]. PiC down-regulation decreased the ATP/ADP ratio in the presence of high glucose, which causes insufficient closure of K_{ATP} channels, a decrease in $[Ca^{2+}]_i$ elevation by glucose (Figures 3A and 3B), and suppression of GSIS (Figure 2).

Insulin secretion at 10 mM glucose was similar to that at 30 mM K^+ and 2 mM glucose in the control samples. In contrast, in PiC down-regulated INS-1 cells, GSIS is lower than depolarization-induced insulin secretion, which suggests specific effects of PiC on metabolism–secretion coupling (Figure 2). However, ~25 % suppression of depolarization-induced insulin secretion, which is modest compared with GSIS, was observed in PiC down-regulated INS-1 cells. Measurements revealed that $[Ca^{2+}]_i$ in the presence of 2 mM glucose and 30 mM K^+ was reduced by PiC down-regulation (Figures 3C and 3D), which plays a role in reduced depolarization-induced insulin secretion by PiC down-regulation. Depolarization reduced the ATP/ADP ratio in the presence of a basal level of glucose in control samples, which accords with a previous study where an increase in $[Ca^{2+}]_i$ causes a larger consumption than production of ATP [24] (Table 2B). The ATP/ADP ratio was also reduced by depolarization at 2 mM glucose in PiC down-regulated INS-1 cells, although the suppression was lower than that in control samples, which may reflect a smaller elevation of $[Ca^{2+}]_i$ than in the control. In addition, in contrast with a significant suppression of the ATP/ADP ratio at high glucose concentrations by PiC down-regulation, in the presence of a basal

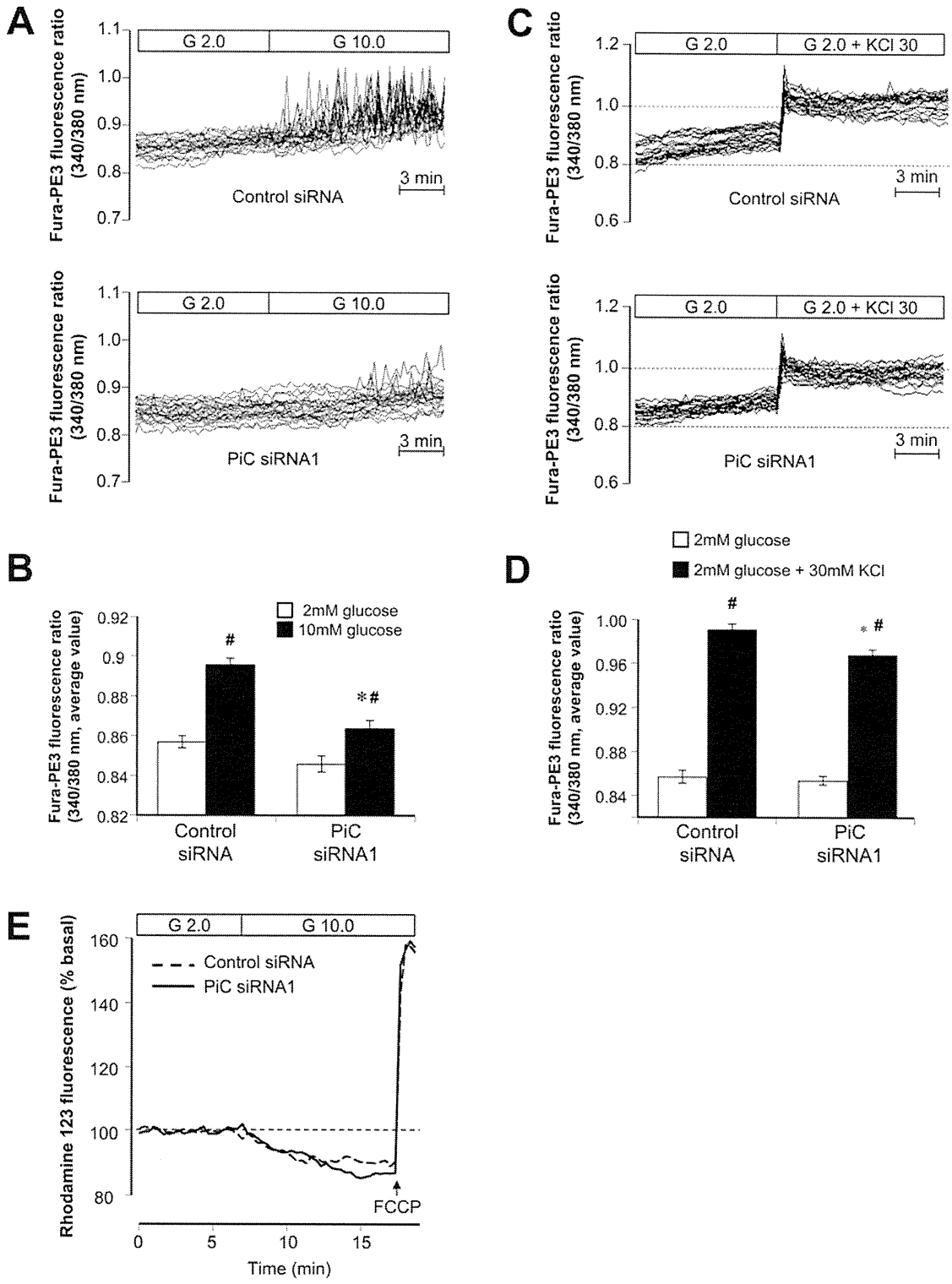

Figure 3 Effects of PiC down-regulation on $[Ca^{2+}]_i$ and $\Delta\psi_m$ in living cells

(**A**) $[Ca^{2+}]_i$ elevation and oscillation induced by raising glucose (G) from 2 to 10 mM were monitored in INS-1 cells transfected with PiC siRNA. Traces of Fura-PE3 fluorescence ratio (340/380 nm) were obtained from 20 cells of each group. (**B**) Average values calculated from the data from (**A**). $*P < 0.01$ compared with control siRNA at 10 mM glucose. $\#P < 0.01$ compared with corresponding 2 mM glucose. (**C**) $[Ca^{2+}]_i$ elevation induced by 30 mM KCl was monitored in INS-1 cells transfected with PiC siRNA. Traces of Fura-PE3 fluorescence ratio (340/380 nm) were obtained from 20 cells of each group. (**D**) Average values calculated from the data from (**C**). $*P < 0.05$ compared with control siRNA at 30 mM KCl. $\#P < 0.01$ compared with corresponding 2 mM glucose. (**E**) $\Delta\psi_m$ monitored by rhodamine 123 fluorescence in INS-1 cells. Data were corrected with the average values of fluorescence under basal glucose (2 mM) conditions. $n = 10$. Error bars are means±S.E.M.

Table 2 Effects of PiC down-regulation on adenine nucleotides

(A)

	Control siRNA		PiC siRNA1		PiC siRNA2	
Glucose (mM)	2	10	2	10	2	10
ATP (nmol/mg protein)	65.2 ± 3.8	77.4 ± 3.8*	64.4 ± 1.0	71.8 ± 3.3*	66.2 ± 1.7	80.0 ± 5.5*
ADP (nmol/mg protein)	10.2 ± 0.6	3.9 ± 0.4†	10.6 ± 0.6	6.4 ± 0.9*‡	9.7 ± 0.6	6.1 ± 1.2*‡
ATP/ADP	6.5 ± 0.6	20.5 ± 2.0†	6.1 ± 0.4	12.0 ± 1.7*‡	6.9 ± 0.5	13.9 ± 1.4*‡

(B)

	Control siRNA			PiC siRNA1	
Glucose (mM)	2	2	2	2	2
K^+ (mM)	3.6	30	3.6	3.6	30
Antimycin A (μM)	0	0	1	0	0
ATP (nmol/mg protein)	65.5 ± 3.4	48.6 ± 1.9*	2.5 ± 0.1†	64.4 ± 4.7	61.2 ± 1.8‡
ADP (nmol/mg protein)	10.1 ± 0.1	11.2 ± 0.2*	10.5 ± 0.1*	9.9 ± 0.2	10.5 ± 0.3*‡
ATP/ADP	6.5 ± 0.3	4.4 ± 0.2†	0.2 ± 0.0†	6.5 ± 0.5	5.8 ± 0.2*§

*$P < 0.05$ and †$P < 0.01$ compared with basal condition (2 mM glucose). ‡$P < 0.05$ and §$P < 0.01$ compared with control siRNA. Data were obtained from four independent experiments.

Table 3 Silencing effects of PiC siRNAs on ATP production from mitochondrial fraction of INS-1 cells

	Mitochondrial ATP production (μmol/10 min per mg of protein)		
Experimental conditions	Control siRNA	PiC siRNA1	PiC siRNA2
1 mM succinate	1.28 ± 0.02	0.61 ± 0.02*	0.46 ± 0.01*
1 mM succinate + 1 μM rotenone	1.03 ± 0.09	0.56 ± 0.03*	0.39 ± 0.01*
1 mM succinate + 1 μM antimycin A	0.03 ± 0.01	0.00 ± 0.01	0.00 ± 0.01
1 mM pyruvate + 1 mM malate	0.41 ± 0.03	0.24 ± 0.01*	0.17 ± 0.00*
0.5 mM TMPD + 2 mM ascorbate	3.43 ± 0.09	1.33 ± 0.03*	1.27 ± 0.01*

*$P < 0.01$ compared with control siRNA. Data were obtained from three independent experiments.

level of glucose, PiC down-regulation did not affect the ATP/ADP ratio in INS-1 cells. An incomplete compensatory effect derived from PiC down-regulation, which is valid in a basal supply of substrate to mitochondria but deteriorates in an accelerated supply at high glucose, might save ATP consumption and maintain the basal ratio of ATP/ADP.

PiC, which is required for mitochondrial ATP production, has two isoforms. PiC-A is expressed in skeletal and cardiac muscle whereas PiC-B is expressed ubiquitously. AAC (ATP/ADP carrier), which is also required for mitochondrial ATP production, has isoforms including AAC1 (SLC25A4), AAC2 (SLC25A5) and AAC3 (SLC25A6). Interestingly, these isoforms, except AAC2, expression of which is absent or scarce in most tissues, distribute similarly to the PiC isoforms: AAC1 is expressed in skeletal and cardiac muscle, and AAC3 is expressed ubiquitously. These distributions imply that ubiquitously-expressed PiC-B and AAC3 may meet stable energy requirement, and PiC-A and AAC1, which are expressed exclusively in muscle, meet higher and prompt energy demands for muscle contraction. In the present study, we demonstrate that PiC-B is the dominant isoform of PiC whereas PiC-A is scarcely expressed in INS-1 cells and rat islets (Figure 1A), which may reflect less prompt energy demand in β-cells compared with that in muscles.

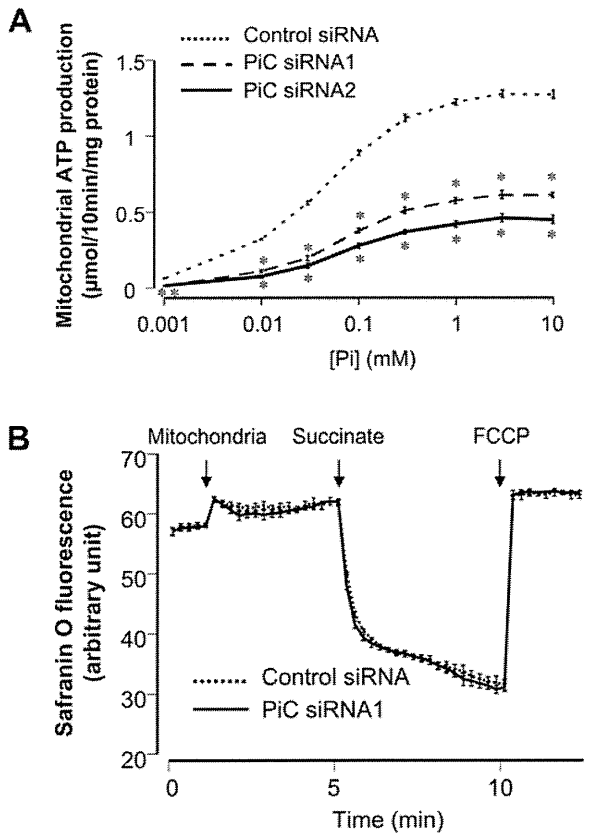

Figure 4 Effects of PiC down-regulation on ATP production and $\Delta\psi_m$ in mitochondrial fraction isolated from INS-1 cells

(**A**) Effects of PiC down-regulation on mitochondrial ATP production at various phosphate concentrations. ATP production was evaluated in mitochondria isolated from INS-1 cells in the presence of 50 μM ADP, 1 μM DAPP and 1 mM succinate with various concentrations of P_i indicated in the Figure. $n = 3$ in each plot. *$P < 0.01$ compared with control siRNA. (**B**) $\Delta\psi_m$ monitored by Safranin O fluorescence. Mitochondria (50 μg/ml), succinate (1 mM) and FCCP (200 nM) were added to the solution containing Safranin O at the points indicated with arrows. $n = 4$ in each group.

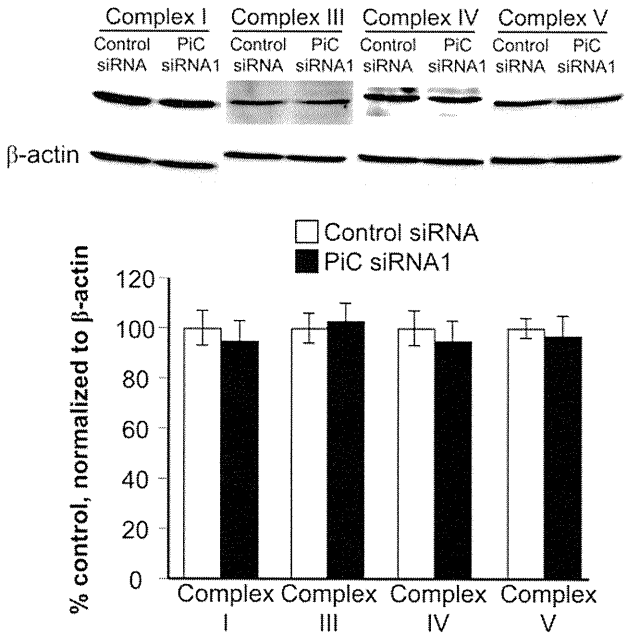

Figure 5 Effects of PiC silencing on expression of mitochondrial respiratory chain proteins

Lysates of whole INS-1 cells were electrophoresed and immunoblotted using antibodies against complex I, III, IV and V. Quantification data were obtained from four independent experiments and normalized with β-actin levels. Error bars are means±S.E.M.

Mitochondrial ATP is produced by complex V (ATP synthase), which is driven by protonmotive force generated by proton extrusion during transport of high-energy electrons in the respiratory chain. In the present study, mitochondrial ATP production in the presence of mitochondrial fuel increased according to the raised extramitochondrial phosphate concentration ($[P_i]_e$), and reached maximum rate above ~3 mM of $[P_i]_e$, which was decreased by 50–60 % without affecting the K_m value of $[P_i]_e$ for ATP production by ~40 % reduction in PiC protein. The physiological intracellular $[P_i]$ in heart determined by methods including ^{31}P NMR is ~1 mM at rest and increases to ~10 mM depending on the metabolic state [25–27]. Levels of P_i in islets are ~20 mmol/kg of dry weight tissue [28], which corresponds to ~10 mM by conversion [29]. Taken together, the rate of mitochondrial ATP production might be barely affected by a physiological change of $[P_i]_e$ but be evidently affected by alteration of the amount of PiC protein. In addition, reduction in ATP production by down-regulation of PiC also suggests that compensatory supply of P_i to mitochondria by other mitochondrial phosphate carriers including DIC (SLC25A10) [30,31] does not occur, which is supported by no apparent effect of PiC down-regulation on DIC expression (Figure 1E). These results accord with the first description that PiC dysfunction impairs the synthesis of ATP [15].

Intramitochondrial P_i is thought to affect oxidative phosphorylation at multiple sites [16]. To find specific defective sites in the respiratory chain in PiC down-regulated INS-1 cells, mitochondrial ATP production was examined in the presence of various substrates and inhibitors. Pyruvate and malate, which are metabolized in mitochondria to generate NADH, render electrons at complex I. In the presence of rotenone, a complex I inhibitor, succinate renders electrons directly to complex II via $FADH_2$. TMPD is an artificial electron donor that can transfer electrons to cytochrome *c*. TMPD reduced by ascorbate renders electrons to cytochrome *c*, which transfers electrons to complex IV. Reduction of ATP production by down-regulation of PiC in the presence of pyruvate plus malate, succinate plus rotenone and TMPD plus ascorbate were all suppressed similarly by 50–60 % (Table 3). These results indicate that reduction in ATP production by down-regulation of PiC may well be derived from a defective site downstream of complex IV and that a defective site upstream of complex IV, if present, does not play a prominent role. Moreover, immunoblotting revealed that expressions of respiratory chain proteins including complex I, III, IV and V were not affected by PiC silencing. Considered together, silencing of PiC seems to suppress mitochondrial ATP production not by affecting mitochondrial biogenesis, but by restricting P_i supply to complex V.

Inhibition of complex V by oligomycin reduces ATP production with hyperpolarization of $\Delta\psi_m$ [32,33], which may be derived from the fact that complex V is a protonophore and its inhibition affects electrogenic H^+ influx to mitochondria specifically and directly affects $\Delta\psi_m$. In contrast, PiC is electroneutral due to symport of H^+ and negatively charged P_i or antiport of OH^- and negatively charged P_i and does not directly affect $\Delta\psi_m$. ATP generation in complex V is driven by protonmotive force (Δp), which has two components: electrical membrane potential ($\Delta\psi_m$) and the difference between the cytosolic and matrix pH (ΔpH) [34,35]. P_i plays regulatory roles in oxidative phosphorylation by affecting Δp. An increase in $[P_i]_e$ reduces ΔpH [34,36–38] due to an increase in co-transport of P_i and protons from cytosol into mitochondrial matrix through PiC. On the other hand, $\Delta\psi_m$ is increased by an increase in $[P_i]_e$ of less than ~2 mM, but reaches a plateau at $[P_i]_e$ above ~2 mM [16,34,38]. Increases in $\Delta\psi_m$ owing to increases in $[P_i]_e$ is not fully elucidated, but some explanations are proposed. An electroneutral influx of protons (H^+) accompanying negatively charged substrates such as P_i does not directly affect $\Delta\psi_m$ but produces a reduction in ΔpH that promotes proton extrusion by the respiratory chain to maintain Δp and eventually increases $\Delta\psi_m$ [35]. Bose et al. [16] provided another explanation: an increase in the influx of P_i activates intramitochondrial NADH production and NADH supply to complex I and also promotes the ability to generate Δp by improving the coupling of electron transport between cytochrome *b* and cytochrome *c*, which eventually increases $\Delta\psi_m$. Interestingly, in the present study, ~40 % reduction in the protein level of PiC did not affect glucose-induced hyperpolarization of the mitochondrial inner membrane in spite of a reduction in ATP production. It is possible that the reduction in P_i influx by down-regulation of PiC in the present study is within a range of P_i influx which does not affect $\Delta\psi_m$ as with higher $[P_i]_e$. In addition, our results were derived from sustained down-regulation of P_i influx to mitochondria, as experiments were performed 48 h after transfection of PiC siRNA in contrast with the acute alteration of P_i influx by manipulation of $[P_i]_e$ in previous studies, which may permit adaptation of $\Delta\psi_m$ to maintain Δp.

It has been generally reported that the contribution of $\Delta\psi_m$ to Δp is 80–85 % [34,35,37–45] or more [16] and that of ΔpH is relatively small, which indicates that the alteration in Δp by down-regulation of PiC in the present study is small considering the non-detectable affect on $\Delta\psi_m$. Therefore the supply of P_i to complex V may well be a critical rate-limiting step for ATP production independent of Δp. The results in the present study demonstrate the critical role of P_i influx to mitochondria in ATP production and metabolism–secretion coupling in pancreatic β-cells.

AUTHOR CONTRIBUTION

Yuichi Nishi researched data, contributed to the discussion, wrote the manuscript and revised/edited the manuscript. Shimpei Fujimoto contributed to the discussion, wrote the manuscript and revised/edited the manuscript. Mayumi Sasaki, Eri Mukai, Hiroki Sato, Yuichi Sato, Yumiko Tahara and Yasuhiko Nakamura researched data. Nobuya Inagaki contributed to the discussion and revised/edited the manuscript.

ACKNOWLEDGEMENTS

We greatly appreciate the gifts of INS-1 cells from Dr Nobuo Sekine (Tokyo Kosei Nenkin Hospital, Tokyo, Japan) and pHMCA5 vector from Dr Hiroyuki Mizuguchi (National Institute of Biomedical Innovation, Ibaraki, Japan). We thank Mr Shinsaku Akagi, Mr Takuro Yamaguchi, Ms Chiyo Kotake and Ms Sara Yasui for technical assistance and Mr Eiji Yoshihara for helpful advice on siRNA transfection.

FUNDING

This study was supported by a Research Grant on Nanotechnical Medicine from the Ministry of Health, Labour, and Welfare of Japan, Scientific Research Grants, a grant from Innovation Cluster Kansai project of the Ministry of Education, Culture, Sports, Science and Technology of Japan, and a grant from CREST (Core Research for Evolutional Science and Technology) of Japan Science and Technology Cooperation.

REFERENCES

1 Maechler, P. and Wollheim, C. B. (2001) Mitochondrial function in normal and diabetic β-cells. Nature **414**, 807–812
2 Kennedy, E. D., Maechler, P. and Wollheim, C. B. (1998) Effects of depletion of mitochondrial DNA in metabolism secretion coupling in INS-1 cells. Diabetes **47**, 374–380
3 Tsuruzoe, K., Araki, E., Furukawa, N., Shirotani, T., Matsumoto, K., Kaneko, K., Motoshima, H., Yoshizato, K., Shirakami, A., Kishikawa, H. et al. (1998) Creation and characterization of a mitochondrial DNA-depleted pancreatic β-cell line: impaired insulin secretion induced by glucose, leucine, and sulfonylureas. Diabetes **47**, 621–631
4 Palmieri, F. (2004) The mitochondrial transporter family (SLC25): physiological and pathological implications. Pflugers Arch. **447**, 689–709
5 Rubi, B., del Arco, A., Bartley, C., Satrustegui, J. and Maechler, P. (2004) The malate-aspartate NADH shuttle member Aralar1 determines glucose metabolic fate, mitochondrial activity, and insulin secretion in beta cells. J. Biol. Chem. **279**, 55659–55666
6 Casimir, M., Rubi, B., Frigerio, F., Chaffard, G. and Maechler, P. (2009) Silencing of the mitochondrial NADH shuttle component aspartate-glutamate carrier AGC1/Aralar1 in INS-1E cells and rat islets. Biochem. J. **424**, 459–466
7 Chan, C. B., MacDonald, P. E., Saleh, M. C., Johns, D. C., Marban, E. and Wheeler, M. B. (1999) Overexpression of uncoupling protein 2 inhibits glucose-stimulated insulin secretion from rat islets. Diabetes **48**, 1482–1486
8 Zhang, C. Y., Baffy, G., Perret, P., Krauss, S., Peroni, O., Grujic, D., Hagen, T., Vidal-Puig, A. J., Boss, O., Kim, Y. B. et al. (2001) Uncoupling protein-2 negatively regulates insulin secretion and is a major link between obesity, β cell dysfunction, and type 2 diabetes. Cell **105**, 745–755
9 Odegaard, M. L., Joseph, J. W., Jensen, M. V., Lu, D., Ilkayeva, O., Ronnebaum, S. M., Becker, T. C. and Newgard, C. B. (2010) The mitochondrial 2-oxoglutarate carrier is part of a metabolic pathway that mediates glucose- and glutamine-stimulated insulin secretion. J. Biol. Chem. **285**, 16530–16537
10 Joseph, J. W., Jensen, M. V., Ilkayeva, O., Palmieri, F., Alarcon, C., Rhodes, C. J. and Newgard, C. B. (2006) The mitochondrial citrate/isocitrate carrier plays a regulatory role in glucose-stimulated insulin secretion. J. Biol. Chem. **281**, 35624–35632
11 Casimir, M., Lasorsa, F. M., Rubi, B., Caille, D., Palmieri, F., Meda, P. and Maechler, P. (2009) Mitochondrial glutamate carrier GC1 as a newly identified player in the control of glucose-stimulated insulin secretion. J. Biol. Chem. **284**, 25004–25014
12 Dolce, V., Iacobazzi, V., Palmieri, F. and Walker, J. E. (1994) The sequences of human and bovine genes of the phosphate carrier from mitochondria contain evidence of alternatively spliced forms. J. Biol. Chem. **269**, 10451–10460
13 Fiermonte, G., Dolce, V. and Palmieri, F. (1998) Expression in *Escherichia coli*, functional characterization, and tissue distribution of isoforms A and B of the phosphate carrier from bovine mitochondria. J. Biol. Chem. **273**, 22782–22787
14 Dolce, V., Fiermonte, G. and Palmieri, F. (1996) Tissue-specific expression of the two isoforms of the mitochondrial phosphate carrier in bovine tissues. FEBS Lett. **399**, 95–98
15 Mayr, J. A., Merkel, O., Kohlwein, S. D., Gebhardt, B. R., Böhles, H., Fötschl, U., Koch, J., Jaksch, M., Lochmüller, H. and Horváth, R. et al. (2007) Mitochondrial phosphate-carrier deficiency: a novel disorder of oxidative phosphorylation. Am. J. Hum. Genet. **80**, 478–484
16 Bose, S., French, S., Evans, F. J., Joubert, F. and Balaban, R. S. (2003) Metabolic network control of oxidative phosphorylation: multiple roles of inorganic phosphate. J. Biol. Chem. **278**, 39155–39165
17 Fujimoto, S., Ishida, H., Kato, S., Okamoto, Y., Tsuji, K., Mizuno, N., Ueda, S., Mukai, E. and Seino, Y. (1998) The novel insulinotropic mechanism of pimobendan: direct enhancement of the exocytotic process of insulin secretory granules by increased Ca^{2+} sensitivity in β-cells. Endocrinology **139**, 1133–1140
18 Takehiro, M., Fujimoto, S., Shimodahira, M., Shimono, D., Mukai, E., Nabe, K., Radu, R. G., Kominato, R., Aramaki, Y., Seino, Y. and Yamada, Y. (2005) Chronic exposure to β-hydroxybutyrate inhibits glucose-induced insulin release from pancreatic islets by decreasing NADH contents. Am. J. Physiol. **288**, E372–E380
19 Schultz, V., Sussman, I., Bokvist, K. and Tornheim, K. (1993) Bioluminometric assay of ADP and ATP at high ATP/ADP ratios: assay of ADP after enzymatic removal of ATP. Anal. Biochem. **215**, 302–304
20 Votyakova, T. V. and Reynolds, I. J. (2001) $\Delta\psi_m$-Dependent and -independent production of reactive oxygen species by rat brain mitochondria. J. Neurochem. **79**, 266–277
21 Leung, A. W., Varanyuwatana, P. and Halestrap, A. P. (2008) The mitochondrial phosphate carrier interacts with cyclophilin D and may play a key role in the permeability transition. J. Biol. Chem. **283**, 26312–26323
22 Detimary, P., Gilon, P., Nenquin, M. and Henquin, J. C. (1994) Two sites of glucose control of insulin release with distinct dependence on the energy state in pancreatic B-cells. Biochem. J. **297**, 455–461
23 Detimary, P., Van den Berghe, G. and Henquin, J. C. (1996) Concentration dependence and time course of the effects of glucose on adenine and guanine nucleotides in mouse pancreatic islets. J. Biol. Chem. **271**, 20559–20565
24 Detimary, P., Gilon, P. and Henquin, J. C. (1998) Interplay between cytoplasmic Ca^{2+} and the ATP/ADP ratio: a feedback control mechanism in mouse pancreatic islets. Biochem. J. **333**, 269–274
25 Katz, L. A., Swain, J. A., Portman, M. A. and Balaban, R. S. (1988) Intracellular pH and inorganic phosphate content of heart *in vivo*: a ^{31}P-NMR study. Am. J. Physiol. **255**, H189–H196
26 Katz, L. A., Swain, J. A., Portman, M. A. and Balaban, R. S. (1989) Relation between phosphate metabolites and oxygen consumption of heart *in vivo*. Am. J. Physiol. **256**, H265–H274
27 Bunger, R., Mallet, R. T. and Hartman, D. A. (1989) Pyruvate-enhanced phosphorylation potential and inotropism in normoxic and postischemic isolated working heart. Near-complete prevention of reperfusion contractile failure. Eur. J. Biochem. **180**, 221–233
28 Ghosh, A., Ronner, P., Cheong, E., Khalid, P. and Matschinsky, F. M. (1991) The role of ATP and free ADP in metabolic coupling during fuel-stimulated insulin release from islet beta-cells in the isolated perfused rat pancreas. J. Biol. Chem. **266**, 22887–22892
29 Erecińska, M., Bryła, J., Michalik, M., Meglasson, M. D. and Nelson, D. (1992) Energy metabolism in islets of Langerhans. Biochim. Biophys. Acta **1101**, 273–295
30 Palmieri, F., Prezioso, G., Quagliariello, E. and Klingenberg, M. (1971) Kinetic study of the dicarboxylate carrier in rat liver mitochondria. Eur. J. Biochem. **22**, 66–74
31 Crompton, M., Palmieri, F., Capano, M. and Quagliariello, E. (1974) The transport of sulphate and sulphite in rat liver mitochondria. Biochem. J. **142**, 127–137
32 Brown, G. C., Lakin-Thomas, P. L. and Brand, M. D. (1990) Control of respiration and oxidative phosphorylation in isolated rat liver cells. Eur. J. Biochem. **192**, 355–362
33 Valdez, L. B., Zaobornyj, T. and Boveris, A. (2006) Mitochondrial metabolic states and membrane potential modulate mtNOS activity. Biochim. Biophys. Acta **1757**, 166–172
34 Dzbek, J. and Korzeniewski, B. (2008) Control over the contribution of the mitochondrial membrane potential ($\Delta\psi$) and proton gradient (ΔpH) to the protonmotive force (Δp). *In silico* studies. J. Biol. Chem. **283**, 33232–33239
35 Martin, D. B. (1995) Bioenergetics. In A Practical Approach (Brown, G. C. and Cooper, C. E., eds), pp. 39–62, Oxford University Press, Oxford
36 Oliveira, G. A. and Kowaltowski, A. J. (2004) Phosphate increases mitochondrial reactive oxygen species release. Free Radic. Res. **38**, 1113–1118
37 Kunz, W., Gellerich, F. N., Schild, L. and Schönfeld, P. (1988) Kinetic limitations in the overall reaction of mitochondrial oxidative phosphorylation accounting for flux-dependent changes in the apparent $\Delta G^{ex}{}_P/\Delta\mu H^+$ ratio. FEBS Lett. **233**, 17–21
38 Nicholls, D. G. (1974) The influence of respiration and ATP hydrolysis on the proton-electrochemical gradient across the inner membrane of rat-liver mitochondria as determined by ion distribution. Eur. J. Biochem. **50**, 305–315
39 Duszyński, J., Bogucka, K. and Wojtczak, L. (1984) Homeostasis of the protonmotive force in phosphorylating mitochondria. Biochim. Biophys. Acta **767**, 540–547

40 Ouhabi, R., Rigoulet, M., Lavie, J. L. and Guérin, B. (1991) Respiration in non-phosphorylating yeast mitochondria. Roles of non-ohmic proton conductance and intrinsic uncoupling. Biochim. Biophys. Acta **1060**, 293–298
41 Czyż, A., Szewczyk, A., Nałcz, M. J. and Wojtczak, L. (1995) The role of mitochondrial potassium fluxes in controlling the protonmotive force in energized mitochondria. Biochem. Biophys. Res. Commun. **210**, 98–104
42 Rigoulet, M., Fraisse, L., Ouhabi, R., Guerin, B., Fontaine, E. and Leverve, X. (1990) Flux-dependent increase in the stoichiometry of charge translocation by mitochondrial ATPase/ATP synthase induced by almitrine. Biochim. Biophys. Acta **1018**, 91–97
43 Hafner, R. P., Brown, G. C. and Brand, M. D. (1990) Analysis of the control of respiration rate, phosphorylation rate, proton leak rate and protonmotive force in isolated mitochondria using the 'top-down' approach of metabolic control theory. Eur. J. Biochem. **188**, 313–319
44 Lambert, A. J. and Brand, M. D. (2004) Superoxide production by NADH:ubiquinone oxidoreductase (complex I) depends on the pH gradient across the mitochondrial inner membrane. Biochem. J. **382**, 511–517
45 Nobes, C. D., Brown, G. C., Olive, P. N. and Brand, M. D. (1990) Non-ohmic proton conductance of the mitochondrial inner membrane in hepatocytes. J. Biol. Chem. **265**, 12903–12909

Received 19 October 2010/21 January 2011; accepted 25 January 2011
Published as BJ Immediate Publication 25 January 2011, doi:10.1042/BJ20101708

GLP-1 receptor agonist attenuates endoplasmic reticulum stress-mediated β-cell damage in Akita mice

Shunsuke Yamane[1], Yoshiyuki Hamamoto[2], Shin-ichi Harashima[1], Norio Harada[1], Akihiro Hamasaki[1], Kentaro Toyoda[1], Kazuyo Fujita[1], Erina Joo[1], Yutaka Seino[3], Nobuya Inagaki[1,4]*

ABSTRACT

Aims/Introduction: Endoplasmic reticulum (ER) stress is one of the contributing factors in the development of type 2 diabetes. To investigate the cytoprotective effect of glucagon-like peptide 1 receptor (GLP-1R) signaling *in vivo*, we examined the action of exendin-4 (Ex-4), a potent GLP-1R agonist, on β-cell apoptosis in Akita mice, an animal model of ER stress-mediated diabetes.

Materials and Methods: Ex-4, phosphate-buffered saline (PBS) or phlorizin were injected intraperitoneally twice a day from 3 to 5 weeks-of-age. We evaluated the changes in blood glucose levels, bodyweights, and pancreatic insulin-positive area and number of islets. The effect of Ex-4 on the numbers of C/EBP-homologous protein (CHOP)-, TdT-mediated dUTP-biotin nick-end labeling (TUNEL)- or proliferating cell nuclear antigen-positive β-cells were also evaluated.

Results: Ex-4 significantly reduced blood glucose levels and increased both the insulin-positive area and the number of islets compared with PBS-treated mice. In contrast, there was no significant difference in the insulin-positive area between PBS-treated mice and phlorizin-treated mice, in which blood glucose levels were controlled similarly to those in Ex-4-treated mice. Furthermore, treatment of Akita mice with Ex-4 resulted in a significant decrease in the number of CHOP-positive β-cells and TUNEL-positive β-cells, and in CHOP mRNA levels in β-cells, but there was no significant difference between the PBS-treated group and the phlorizin-treated group. Proliferating cell nuclear antigen staining showed no significant difference among the three groups in proliferation of β-cells.

Conclusions: These data suggest that Ex-4 treatment can attenuate ER stress-mediated β-cell damage, mainly through a reduction of apoptotic cell death that is independent of lowered blood glucose levels. (J Diabetes Invest, doi: 10.1111/j.2040-1124.2010.00075.x, 2011)

KEY WORDS: Apoptosis, Endoplasmic reticulum stress, Glucagon-like peptide-1

INTRODUCTION

Type 2 diabetes is a chronic metabolic disorder characterized by the loss of β-cell function and mass. The mechanisms underlying the loss of β-cell function and mass are not fully understood, but recent studies have shown that endoplasmic reticulum (ER) stress is one of the causes of β-cell damage in diabetes[1]. Owing to increased demand for insulin secretion, β-cells show a highly developed ER[1]. The ER has a number of important functions, such as post-translational modification, folding and assembly of newly synthesized secretory proteins[2–4]. Thus, the ER plays an essential role in cell survival. ER function can be impaired by various conditions, including inhibition of protein glycosylation, reduction in formation of disulfide bonds, calcium depletion from the ER lumen, impairment of protein transport from the ER to the Golgi and expression of malfolded proteins[1]. Various physiological or pathological conditions that compromise ER functions are collectively termed ER stress[1–3]. To alleviate ER stress and promote cell survival, an adaptive response, known as unfolded protein response (UPR) is activated. UPR comprises translational attenuation, induction of chaperones and ER stress-associated degradation (ERAD). However, prolonged activation of UPR can ultimately lead to cell death by apoptosis.

Increased demand for insulin secretion under certain conditions, such as chronic hyperglycemia, might result in β-cell overload. Chronic hyperglycemia in diabetes can therefore induce persistent ER stress, cause β-cell dysfunction and finally lead to a reduction in β-cell mass through apoptosis[1].

Glucagon-like peptide 1 (GLP-1) is a physiological incretin, an intestinal hormone released in response to nutrient

[1]Department of Diabetes and Clinical Nutrition, Graduate School of Medicine, Kyoto University, [4]CREST of Japan Science and Technology (JST), Kyoto, [2]Center for Diabetes and Endocrinology, Tazuke Kofukai Medical Research Institute, Kitano Hospital, and [3]Division of Diabetes, Clinical Nutrition and Endocrinology, Department of Medicine, Kansai Electric Power Hospital, Osaka, Japan
*Corresponding author. Nobuya Inagaki Tel.: +81 75 751 3562 Fax: +81 75 771 6601
E-mail address: inagaki@metab.kuhp.kyoto-u.ac.jp
Received 21 July 2010; revised 25 August 2010; accepted 8 September 2010

ingestion that stimulates glucose-dependent insulin secretion. A growing body of evidence suggests that GLP-1 not only increases insulin secretion and upregulates insulin biosynthesis, but also stimulates β-cell proliferation and neogenesis[5–9], and inhibits β-cell apoptosis[9–16], resulting in increased β-cell mass. However, demonstration of an *in vivo* effect in the animal models of type 2 diabetes is problematic, because enhancement of GLP-1R signaling lowers blood glucose levels as result of its insulinotropic action, and it is difficult to evaluate the direct cytoprotective effects of GLP-1 in conditions of similar glucose toxicity.

In the present study, we investigated the cytoprotective effect of GLP-1R signaling *in vivo* on ER stress-mediated apoptotic cell death by using Akita mice, an animal model of ER stress-mediated diabetes mellitus. Akita mice have a point mutation in the insulin 2 gene, resulting in misfolding of insulin that leads to severe ER stress[17,18]. To exclude the possibility that the effect of Ex-4 on β-cells is mediated through improved blood glucose levels, we used three groups of mice: Akita mice treated with phosphate-buffered saline (PBS), Ex-4, or the sodium-coupled glucose transporter inhibitor phlorizin, which decreases blood glucose levels without increasing insulin secretion.

MATERIALS AND METHODS

Experimental Animals

Male C57BL/6 mice and male Akita mice were obtained from Shimizu (Kyoto, Japan). The animals were housed under a light/dark cycle of 12 h with free access to food and water. All experiments were approved by the Kyoto University Animal Care Committee.

In vivo Treatment

The mice were given twice daily intraperitoneal injections of PBS, Ex-4 (24 nmol/kg) or phlorizin (0.3 g/kg) for 2 weeks (from 3 to 5 weeks-of-age). Blood glucose levels were measured every third day by enzyme electrode method using a portable glucose analyzer (Glutest sensor; Sanwakagaku, Nagoya, Japan). Blood samples were collected from tail cuttings from these mice fed *ad libitum*. At the end of the experimental period, blood samples were collected from the inferior vena cava under anesthesia to determine the plasma glycoalbumin levels (Oriental Yeast, Tokyo, Japan). Pancreas samples from each of the animal groups were obtained for histological evaluation, and islets were isolated for measurement of insulin content and RNA extraction.

Evaluation of Pancreatic Insulin-Positive Area and Number of Islets

The pancreas samples were fixed in Bouin's solution. Serial 5-μm paraffin-embedded tissue sections were mounted on slides. After rehydration, sections were incubated with polyclonal rabbit anti-insulin antibodies (Santa Cruz Biotechnology, Santa Cruz, CA, USA), with a biotinylated goat anti-rabbit antibody (DAKO, Carpinteria, CA, USA), and then with a streptavidin peroxidase conjugate and substrate kit (DAKO) using standard protocols. The total pancreas area and insulin-positive area were quantified on five distal, random, non-overlapping sections from five mice of each group using a BZ-8100 microscope equipped with a BZ-Analyzer (KeyEnce, Osaka, Japan). Insulin-positive areas and the number of islets of each group were adjusted by total pancreas area[15].

Measurement of Insulin Contents of Isolated Islets

Pancreatic islets were isolated by collagenase digestion. To determine insulin contents, islets were homogenized in 400 μL acid ethanol (37% HCl in 75% ethanol, 15:1000 [v/v]) and extracted at 4°C overnight. The acidic extracts were dried by vacuum, reconstituted and subjected to insulin measurement. The amount of immunoreactive insulin was determined by radioimmunoassay (RIA).

Measurement of mRNA Expression of C/EBP-Homologous Protein and BiP in Isolated Islets

Measurement of mRNA expression of C/EBP-homologous protein (CHOP) and BiP was carried out by quantitative reverse transcription polymerase chain reaction (RT–PCR) as described previously[19]. Briefly, total RNA was extracted from isolated islets with an RNeasy mini kit (Qiagen, Valencia, CA, USA) and treated with DNase (Qiagen). cDNA was prepared by SuperScript Reverse Transcriptase system (Invitrogens, Carlsbad, CA, USA) according to the manufacturer's instructions. CHOP mRNA levels and BiP mRNA levels in the islets were measured by quantitative RT–PCR using an ABI PRISM 7000 Sequence Detection System (Applied Biosystems, Foster City, CA, USA). The sequences of forward and reverse primers to evaluate

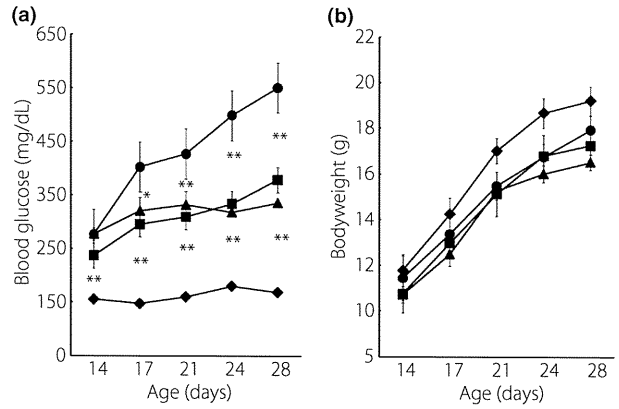

Figure 1 | Ex-4 significantly reduced blood glucose levels in Akita mice. (a) Blood glucose concentration and (b) bodyweight were measured in wild-type C56BL/6 mice (closed diamond, $n = 10$), Akita mice treated with PBS alone (closed circle, $n = 10$), Ex-4 (closed square, $n = 12$) and phlorizin (closed triangle, $n = 10$). Each symbol represents mean ± SE. $^*P < 0.05$, $^{**}P < 0.01$ *vs* PBS-treated Akita mice.

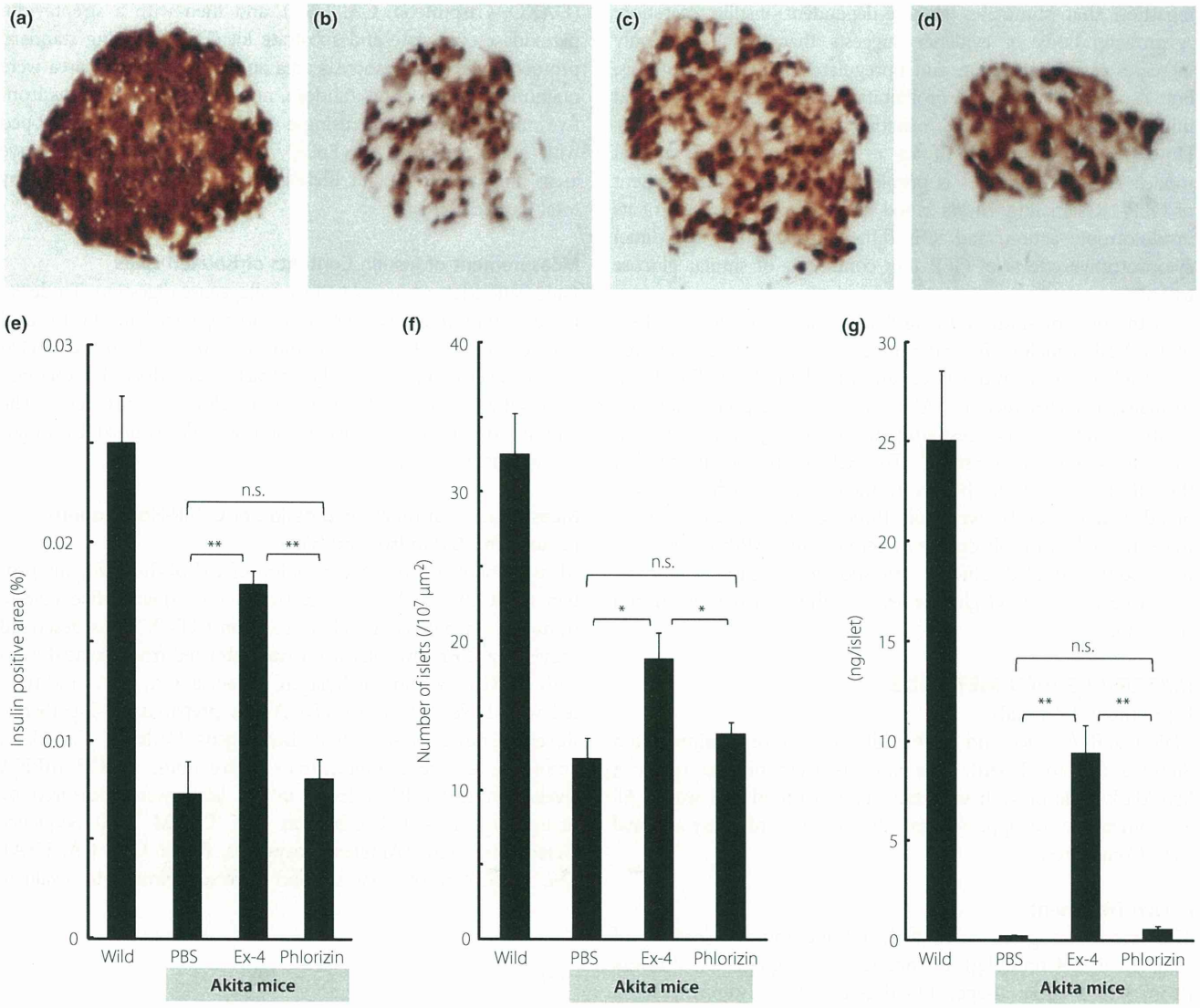

Figure 2 | Ex-4 treatment increased insulin-positive areas, number of islets and insulin content. (a–d) Representative mouse pancreata at 5 weeks-of-age stained with insulin. (a) Wild, (b) Akita mice treated with PBS, (c) Ex-4 or (d) phlorizin. (e) Insulin-positive areas and (f) number of islets were evaluated as described in Materials and Methods (n = 5 for each group). (g) Pancreatic insulin content was measured as described in Materials and Methods, and expressed as ng/islet (n = 5 for each group). Each column represents mean ± SE. *P < 0.05, **P < 0.01.

CHOP expression were 5′-GAGCT- GGAAGCCTGGTATGA-3′ and 5′-GGACGCAGGGTCAAGAGTAG-3′, respectively; the sequences of forward and reverse primers to evaluate BiP expression were 5′-TTTCTGCCATGGTTCTCACTAA-3′ and 5′-GCTGGGCATCATTGAAGTAAG-3′, respectively; and the sequences of forward and reverse primers to evaluate glyceraldehyde 3-phosphate dehydrogenase (GAPDH) expression were 5′-AGCTCACTGGCATGGCTTCCG-3′ and 5′-GCCTGCTTC-ACCACCTTCTTGATG-3′, respectively. SYBER Green PCR Master Mix (Applied Biosystems) was prepared for the PCR run. Thermal cycling conditions were denatured at 95°C for 10 min followed by 50 cycles at 95°C for 15 s and 60°C for 1 min. Total CHOP and total BiP levels were corrected by GAPDH mRNA levels.

Immunofluorescence Staining

For pancreatic CHOP and insulin immunohistochemistry, the tissues were fixed and embedded in paraffin. Serial 5-μm sections were stained with anti-CHOP/GADD153 (Santa Cruz Biotechnology) and anti-insulin (DAKO) antibodies using standard protocols. Insulin immunopositive areas were measured on five distal, random, non-overlapping sections from five mice of each group using a BZ-8100 fluorescence microscope equipped with a BZ-Analyzer (KeyEnce), and the number of cells showing